AR-009-808

DSTO-TR-0399

DSTO

Experimental Results of Cruciform Specimens Under Biaxial Elastic-Plastic Loading

C.H. Wang and M. Heller

APPROVED FOR PUBLIC RELEASE

© Commonwealth of Australia

DTIC QUALITY INSPECTED 4

DEPARTMENT OF DEFENCE

DEFENCE SCIENCE AND TECHNOLOGY ORGANISATION

THE UNITED STATES NATIONAL
TECHNICAL INFORMATION SERVICE
IS AUTHORISED TO
REPRODUCE AND SELL THIS REPORT

DISCLAIMER NOTICE

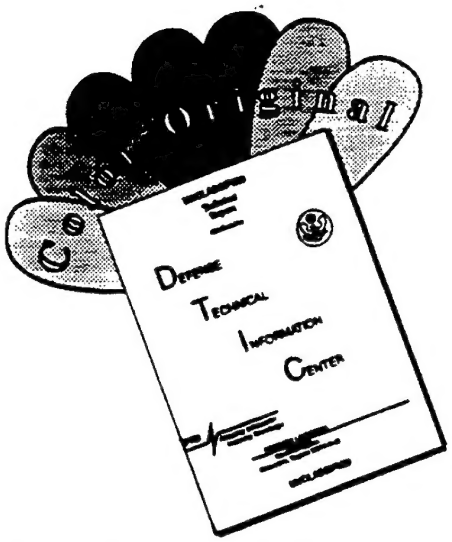

THIS DOCUMENT IS BEST QUALITY AVAILABLE. THE COPY FURNISHED TO DTIC CONTAINED A SIGNIFICANT NUMBER OF COLOR PAGES WHICH DO NOT REPRODUCE LEGIBLY ON BLACK AND WHITE MICROFICHE.

Experimental Results of Cruciform Specimens under Biaxial Elastic-Plastic Loading

C.H. Wang and M. Heller

Airframes and Engines Division
Aeronautical and Maritime Research Laboratory

DSTO-TR-0399

ABSTRACT

Biaxial experiments have been conducted using cruciform specimens to generate elastic-plastic material deformation data. Such data is required to validate a multiaxial constitutive model which has been implemented in finite element analysis codes at AMRL. The elastic-plastic data have been obtained for two aircraft metallic materials namely: 7050 aluminium alloy and D6AC high strength steel. In this work some of the deficiencies in the existing biaxial test system at AMRL have been rectified, including the provision for strain control testing. It has been shown that for this type of work, a new specimen design is needed to allow a wider range of biaxial stress conditions to be investigated, and a suitable design is given herein. Furthermore, as an alternative to incremental plasticity models, a simple closed-form, integral solution has been developed and is presented for proportional, cyclic, loading. Using this integral solution, good agreement between experimental results and the theoretical predictions has been obtained.

RELEASE LIMITATION

Approved for public release

DEPARTMENT OF DEFENCE

DEFENCE SCIENCE AND TECHNOLOGY ORGANISATION

19961217 083

Published by

DSTO Aeronautical and Maritime Research Laboratory
PO Box 4331
Melbourne Victoria 3001

Telephone: (03) 9626 8111
Fax: (03) 9626 8999
© Commonwealth of Australia 1996
AR No. AR-009-808
August 1996

APPROVED FOR PUBLIC RELEASE

Experimental Results of Cruciform Specimens under Biaxial Elastic-Plastic Loading

Executive Summary

Elastic-plastic stress-strain analysis is a vital prerequisite to aircraft structural integrity and durability analysis. In order to perform an accurate analysis of the stress/strain distribution at critical locations in aircraft structures under cyclic loading, an accurate three-dimensional stress-strain (ie constitutive) model is required. Such a model is then typically used in conjunction with a finite element stress analysis. To date, the constitutive model being implemented at AMRL has only been verified using uniaxial data and it is the aim of this work to generate biaxial cyclic deformation data to enable its validation.

This report presents the results of biaxial tests which have been conducted using the AMRL biaxial test rig and a cruciform specimen. As part of this work, the controller for the biaxial test machine has been modified to allow tests to be conducted under strain-controlled conditions. A bending/buckling detecting technique has also been developed to provide additional safety control. As a result of the work undertaken, the biaxial machine is now fully functional, the design of a significantly improved specimen has been completed, and some valuable experimental data have been obtained. A simple closed-form, integral constitutive relation has been developed and presented for proportional, cyclic loading. Using this integral solution, good agreement between experimental results and the theoretical predictions has been obtained.

Authors

C.H. Wang
Airframes and Engines Division

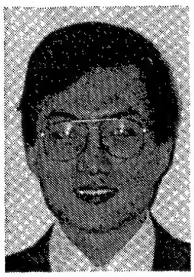

Chun-Hui Wang has a B.Eng and Ph.D (Sheffield, UK) in Mechanical Engineering and is currently a member of the Institute of Engineers, Australia. Prior to joining the Aeronautical and Maritime Research Laboratory in 1995 as a Senior Research Scientist, Dr. Wang was a Lecturer at the Deakin University. He has an extensive research record in fatigue and fracture mechanics, stress analysis and constitutive modelling, and biomechanics. Over the last six years he also held academic/research positions at the University of Sydney and the University of Sheffield, UK.

M. Heller
Airframes and Engines Division

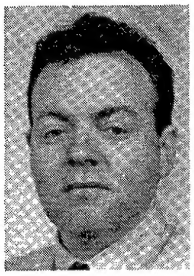

Manfred Heller completed a B. Eng. (Hons.) in Aeronautical Engineering at the University of New South Wales in 1981. He was awarded a Department of Defence Postgraduate Cadetship in 1986, completing a Phd at Melbourne University in 1989. He commenced work in Structures Division at the Aeronautical Research Laboratory in 1982. He has an extensive publication record focussing on the areas of stress analysis, fracture mechanics, fatigue life extension methodologies and experimental validation. Since 1992 he has led tasks which develop and evaluate techniques for extending the fatigue life of ADF aircraft components and provide specialised structural mechanics support to the ADF. He is currently a Senior Research Scientist in the Airframes and Engines Division.

Contents

1. Introduction

In recognition of the need to understand fatigue crack growth behaviour under biaxial stresses, a biaxial test machine has been under development at AMRL-FB [1] over the last decade. More recently, research has been undertaken to model the elastic/plastic deformation behaviour of metals and adhesives under cyclic loading conditions. The reasons for this are legion, and some of the most important aspects include; (i) most key aircraft components and structures in service are subjected to biaxial loading, such as in the F-111C stiffener runout and the fuel flow vent hole. It is known that biaxial loading can be more detrimental than uniaxial loading on the basis of conventional failure criteria, and (ii) there is an urgent need for validating constitutive models adopted for implementation in finite element (FE) codes (the mostly extensively used FE code at AMRL currently is PAFEC). Of particular importance is the characterisation of the biaxial response of two aircraft metallic material, namely: 7050 al-alloy (F/A-18) and D6AC steel (F-111 wing pivot fitting). It is believed that a powerful computational tool, such as a finite element package with a validated advanced constitutive model, will greatly enhance AMRL's capability in handling the elastic/plastic stress-strain distribution at critical locations in RAAF aircraft. So far, however, the constitutive model adopted in the FE code has been verified for uniaxial loading only.

Preliminary tests using the AMRL biaxial test system have been completed. They demonstrate that for the selected design of specimen the desired uniformity of elastic biaxial stress field over the test section of the specimen was achieved. However significant limitations in the machine control system were subsequently encountered, and all these preliminary tests were limited to elastic loading only [2]. Since the main objective of the present biaxial work is to provide input to validate AMRL constitutive model for the D6AC material used in the F-111 aircraft, it was essential to extend the tests into the elastic-plastic region, which would require a reassessment of both specimen design and test machine control configuration.

Consequently the aims of this report are to present (i) the development of an improved test machine control system, and the progress made to date, (ii) closed-form solutions as an alternative to incremental constitutive models, so as to provide a more efficient computational method for determining both uniaxial and multiaxial elastic-plastic deformations, and (iii) a buckling analysis for the cruciform specimens, including a comparison with experimental results.

2. Specimen Design and Experimental Setup

2.1 Specimen Design

The cruciform specimen chosen previously [3] for biaxial verification tests is shown in Figure 1. The specimen is clearly complex and expensive to produce, but was chosen mainly to ensure that a constant, controlled biaxial stress field can be maintained within the test section. After comparing different kinds of cruciform specimen designs using finite element analysis, this design was demonstrated to provide a relatively uniform elastic stress distribution (variation less than 2%) over 70% of the working section [4]. The array of slots machined along each edge of the working area serve two purposes. Firstly they allow a uniform distribution of applied stress along the edge, as each "finger" experiences the same extension or contraction under uniaxial load. Secondly, they minimise specimen strain cross-sensitivity between the two loading axes, since as the load is applied along one axis, the individual fingers on the other loading axis are able to flex relatively freely. This allows the central gauge section to deform with minimum restraint along the edges. Since the edge constraint is small, a uniform distribution of strain is readily obtained over the working section of the specimens from the separate loads applied to each axis.

2.2 Specimen loading conditions

The feature of stress uniformity is important in the study of fatigue crack growth under biaxial loading, since it enables cracks to grow in a uniform stress-field over a wide range of crack lengths, it is however less critical to an investigation of biaxial deformation. The purpose of the relatively thin section (see Figure 1) within the square gauge area was to localise the deformation there, however the possibility of buckling was not properly addressed at the time of design of these specimens, although the possibility was noted [4]. Figure 2 depicts the assembly of a cruciform specimen in the biaxial test machine. Due to the use of long loading arms to extend the actuators (see Figure 2a), alignment was a problem and initially this was overcome by welding the actuator mounts to the test machine frame. However the mounting of specimens still remained a difficult operation, which was exacerbated by the tendency of the vertical actuators to creep down when the hydraulics are turned off. Currently a jack is placed underneath the vertical actuator when the hydraulics is switched to low pressure, before the power is finally switched off.

2.3 Test machine control details

Since the machine was originally designed to run in load control only, (which is not suitable for plastic deformation studies), some modifications have been implemented in the current work programme to convert the system into one which provides for strain control. This would provide better control stability and repeatability, particularly in the high stress regime above the material's yield stress. To achieve this, four active and four dummy strain gauges are attached to the specimen to form two full bridges for the strain control of the machine in both axes, as illustrated in Figure 3. For each full bridge, two active gauges are placed on the two sides of the specimen as per the circuit diagram shown in Figure 4(a). Here, the active gauges on one side are designated A1 and A2 while those on the other side are B1 and B2. The dummy gauges on the two sides are designated as X1, Y1, and X2, Y2 respectively. In addition, four strain gauges are also attached to the specimen (C1, C2 on one side and D1, D2 on the other) to form two half-bridges to monitor any possible bending of the specimen, see Figure 4(b). A predetermined level is set so that the machine would be commanded to cease further loading and ramp slowly from its current load to zero strain, if the mechanical safety switch of the machine is not trigged prior to this. The predetermined limit was initially set at 200 με, but later it was found that the misalignment in the vertical axis caused a 10% difference in the strain gauge readings (indicating a bending strain equal to 5% of the average strain). So a larger safety level was set to enable experiments to run smoothly. This bending monitoring arrangement was also intended as a safety device to stop the test before buckling takes place to protect the specimen. However this was subsequently proven to be impossible as the buckling happens so quickly that there is insufficient time to unload the specimen to avoid buckling; see Section 5.

2.4 Test program

The following tests are proposed to generate stress-strain data for validating the constitutive model: (a) Uniaxial loading, (b) proportional loading with biaxiality ratios equal to $\beta = 0.5$ and $\beta = 2.0$, (c) equi-biaxial loading, (d) shear loading, and (e) plane strain loading. Here the biaxiality ratio is defined as the ratio between the vertical strain and the horizontal strain.

3. Experimental Analysis and Results

The preliminary tests were conducted under load control. The specimens for these tests were manufactured from aluminium alloy 5083, with a strain gauge rosette placed at the centre of each specimen. Subsequently three specimens were manufactured from 7050 Al-alloy and three from D6AC steel. The tests on the D6AC specimens were performed under strain control using the modified control system.

3.1 Specimen alignment

When a specimen is loaded in the horizontal axis only (in this case the vertical axis control is switched off to allow free deformation), the bending strains in both the vertical and horizontal directions are observed to be less than 1% of the applied (average) strain; see Figure 5. Therefore the alignment in the horizontal axis is extremely good. However, when the specimen is loaded in the vertical direction while the horizontal control is switched off, a significant bending strain is observed, about 4.4% of the direct strain; see Figure 6. This suggests that there is slight misalignment in the vertical direction. Assuming the misalignment is δ, the bending strain can be expressed in terms of the direct strain as follows,

$$\frac{6M}{Lh^2E} = \alpha \frac{P}{LhE} \qquad (1)$$

where α is the ratio between the bending strain and the direct strain, which is equal to 0.044 in the present case. Here M represents the bending moment, L and h are the width and thickness of the specimen respectively, and E is the Young's modulus. Since $M=P\delta$, we have

$$\delta = \alpha \frac{h}{6} \qquad (2)$$

Noting that the thickness of the working section is h=2.5 mm, the misalignment is calculated to be about 0.018 mm. Although this misalignment is not significant, considering the long distance between the actuator and the specimen (about 0.5 m), in future work it will be desirable to eradicate this error by adjusting the specimen alignment in the vertical axis.

3.2 Tests of aluminium alloy 5083 Specimens under load control

A total of seven elastic loading cases have been conducted, including uniaxial, equi-biaxial and plane strain. Denoting the biaxiality factor as the ratio between vertical strain and horizontal strain, ie.

$$\beta = \frac{\text{vertical strain}}{\text{horizontal strain}} = \frac{\varepsilon_v}{\varepsilon_h} \qquad (3)$$

the results shown in Figs. 7-13 correspond to β = -0.3, -3.3, 0.5, 2, 1, 0 and ∞, respectively. Due to difficulties with the control system, only valid data in the elastic regime were obtained. The figures show that good linearity between applied load an strain response a the strain gauge locations. It can be seen that there was minimal cross-sensitivity in strain response, for the two loading axes.

Subsequent testing as outlined in section 3.3 used the new strain control system as explained in section 2.3.

3.3 Tests of D6AC steel Specimens under strain control

A total of 14 tests have been carried out, mostly in the elastic region. Some typical biaxial experimental results are shown in Figs. 14-20, corresponding to β = -0.3, -3.3, 0.5, 2, 1, 0, ∞, respectively. The primary purpose of these elastic tests was to verify the satisfactory performance of the machine control system and the computer data acquisition software. The linearity of the elastic results indicate the response of the specimen followed the imposed loading path, through the use of the control software program.

3.4 Cyclic plasticity modelling for proportional loading

In reference [5] elastic/plastic results are given for cylindrical bar specimens under monotonic and cyclic uniaxial loading, these are reproduced in Fig 21a, (depicted by triangular symbols) and those obtained in the present work using the cruciform specimens are also presented in Figure 21a. Taking the basic material properties for D6AC steel as, E=210 GPa and ν=0.32, from reference [6], and making use of the Ramberg-Osgood hardening relationship,

$$\varepsilon = \frac{\sigma}{E} + \left(\frac{\sigma}{K}\right)^{1/n} \qquad (4)$$

the strain hardening coefficient and exponent are equal to 1853 MPa and 0.044 for monotonic loading. The fitted curves are shown as solid lines in Fig 21a.

From reference [5] we have also reproduced the stabilised cyclic stress/strain curve (connecting peak points on stress/strain curves at various constant strain levels). Fitting equation 4 to this curve gives K= 3797 MPa and n=0.194. This is plotted in Fig 21a as the dashed line.

The Masing assumption states that the hysteresis strain hardening is the same as the cyclic stress-strain relationship, thus the cyclic hysteresis loop can be predicted by modifying equation (4) as follows,

$$\varepsilon - \varepsilon^R = \frac{\sigma - \sigma^R}{E} + 2\left(\frac{\sigma - \sigma^R}{2K}\right)^{1/n} \qquad (5)$$

where σ^R and ε^R are the stress and strain at a turning point (the peak point of cyclic curve). Hence using the cyclic stress/strain constants (K= 3797 MPa and n=0.194) and equation (5) we can give a prediction for the hysteresis loop shape, which is shown as a solid line in Figure 21b. For comparison purposes the experimental data for cylindrical and cruciform specimens (for uniaxial loading) are given together with the predictions (dotted line) based on the monotonic constants (K=1853 MPa and n=0.044) for cylindrical specimens. It can be seen there is good agreement between the results generated from different specimens using different test machines.

The approach given above is believed to be valid for uniaxial loading conditions. In the case of proportional biaxial or multiaxial loading conditions, the above method can be extended. This can be achieved by using an integral theory, which is presented in the appendix. Predictions arising from the theory given in the appendix are compared to experimental results in Figure 22. It can be seen that the predicted response correlates well with the experimental data. The plastic strains would be over-estimated if the effect of loading history is ignored and this half cycle is considered as monotonic loading; a prediction is also shown in the figure. It should be noted that general non-proportional loading requires an incremental version [7,8].

4. Buckling Analysis of Cruciform Specimens under Biaxial Compressive Loading

It was expected that specimen buckling would be a problem when a high level load is applied in order to generate plasticity. An analysis has therefore been carried out to assess the critical loading at which the specimen will buckle.

4.1 Theory

The governing differential equation of a square plate under biaxial loading as shown in Figure 23 is, given in reference [9] as,

$$\frac{\partial^4 w}{\partial x^4} + 2\frac{\partial^4 w}{\partial x^2 \partial y^2} + \frac{\partial^4 w}{\partial y^4} = \frac{1}{D}\left(\sigma_x \frac{\partial^2 w}{\partial x^2} + \sigma_y \frac{\partial^2 w}{\partial y^2}\right) \qquad (6)$$

where w is the out-of-plane deflection of the plate, and

$$D = \frac{Eh^2}{12(1-\nu^2)} \qquad (7)$$

where E and ν are respectively the material's Young's modulus and Poisson's ratio, h is the plate thickness, L is the length and width of the plate, and the horizontal and vertical stresses are given by σ_x and σ_y respectively. For a simply supported square plate we have

$$w = \sum_{m=1}^{\infty}\sum_{n=1}^{\infty} w_{mn} \sin\frac{m\pi x}{L}\sin\frac{n\pi y}{L} \qquad (8)$$

Here m and n signify the number of half-waves in the buckled plate in the x and y directions, respectively. For the central section of the specimen we have a length and width of L, and from equations (6) and (8) we therefore have

$$\pi^2 D\left(\frac{m^2}{L^2} + \frac{n^2}{L^2}\right)^2 = -\sigma_x \frac{m^2}{L^2} - \sigma_y \frac{n^2}{L^2} \qquad (9)$$

and so

$$\sigma_x m^2 + \sigma_y n^2 = -(m^2 + n^2)^2 \frac{\pi^2 D}{L^2} \qquad (10)$$

If we take m=1 and n=1, the critical loads at which the central section of the specimen will buckle can be expressed as

$$\sigma_x + \sigma_y = -4\frac{\pi^2 D}{L^2} \qquad (11)$$

Since the arms of the cruciform specimens are much stiffer than the central section, the working area should be considered as fully clamped. Consequently the critical stress that the specimen can sustain might be higher than the above predicted level. In this case, an approximate solution [10] is

$$\sigma_x + \sigma_y = -10.7\frac{\pi^2 D}{L^2} \qquad (12)$$

It can be seen from equations (11) and (12) that the critical stress is approximately 2.6 times that of the simply supported case.

4.2 Steel specimens

For the steel specimens, taking the properties as in section 3.3, and a yield stress of 1200 MPa, the critical stress from equation (12) is plotted in Figure 24. Also given in this Figure is the yield surface for biaxial loading, assuming the von Mises yield condition. Clearly the highest compressive stress that the specimen can sustain under uniaxial loading, for the simply supported case, is about 427 MPa for the dimensions shown in Figure 1, which is far less than the yield stress of the steel specimen. It is also evident that buckling will occur far earlier than yielding, an unsatisfactory situation when the aim of the tests is to generate plasticity in the specimen. Even with the fully clamped end condition, the critical stress is still only 1142 MPa, less than the compressive yield stress of the steel specimen. Under equibiaxial compression ($\sigma_x = \sigma_y$), the buckling load will be further reduced to half the above mentioned value, namely 571 MPa for each loading axis. Hence the current design does not allow a compressive stress sufficiently high to generate plastic deformation, although some limited shear loading ($\sigma_x = -\sigma_y$) tests can be conducted.

During a particular biaxial test, one specimen was first loaded to 10,000 and 5,000 micro strain in the horizontal and vertical axes and then unloaded to zero strain. Just before the zero strain state was reached, the specimen buckled at horizontal and vertical loads of -200 kN and -100 kN, which corresponds to compressive stresses of -744 MPa and -377.5 MPa, respectively. As shown in Figure 24, this result conformed to the present buckling analysis.

4.3 Loading fingers

The 'fingers', formed by the slots and used to apply the load, also raise a concern of possible buckling. Each finger has the following dimensions: length l = 47mm, width a = 4mm, and thickness of b = 7mm. Obviously if the fingers are to buckle, they will occur in the specimen plane. The Euler buckling load for the finger is given by

$$p_{cr} = \frac{\pi^2 EI}{l_e^2} \qquad (13)$$

where p_{cr} represents the critical load of a finger, $I = ab^3/12$, and $l_e = l/2$ for fixed end conditions. For the present case the calculated buckling load is 160 kN. Since there are 12 fingers on each edge, and the maximum possible machine applied load is 440 kN, there is no danger that the fingers will buckle under the testing condition.

4.4 Comments and recommendations

The above analyses indicate that the designed specimens are not suitable for conducting plastic loading tests, especially for positive biaxiality loading. While this type of cruciform specimen has proved successful in biaxial fatigue research, in which a pre-crack is introduced and as a result the overall stress level is normally less than one-third of the material's yield stress (a condition for LEFM to be valid), it is, however, not suitable for high stress loading. For aluminium specimens, where, since the Young's modulus is roughly one third that of the steel, the buckling stress would be about 142 MPa using the analysis of section 3.3. This puts a severe limit on the stress level (thus plastic strain level) that can be applied. One alternative is to use an anti-buckling device to minimise the buckling problem, but since a large area of the working section is strain gauged, this may induce some problems, such as affecting the accuracy of the strain gauge reading. Another option is to increase the cross section thickness, but this would result in requiring a higher test machine loading capacity. Therefore an analysis is required to determine the optimum design parameters for a cruciform specimen capable of sustaining high plastic strain without buckling.

4.5 Improved specimen design

To design a cruciform specimen suitable for elastic-plastic loading, three conditions have to be satisfied, namely

(a) the overall load required to strain the working section to its tensile strength limit should not exceed the machine capacity, viz,

$$Lh \le \frac{P_{max}}{\sigma_f} \tag{14}$$

where P_{max} is the machine overall loading capacity in either axis, and σ_f is the material ultimate tensile strength.

(b) the specimen should not buckle under any combined loading condition;

Since the worst case in terms of buckling is the equibiaxial compression, $\sigma_x = \sigma_y$, the design requirement (b) using equation (12) can be expressed as

$$10.7\pi^2 \frac{D}{L^2} \ge 2\sigma_f \tag{15}$$

Therefore substituting from equation (7), into equation (15) we have,

$$h \ge \frac{L}{\pi}\sqrt{\frac{12(1-\nu^2)\sigma_f}{5.4E}} \tag{16}$$

The variation of h from the two equations, (14) and (16) is plotted in Figure 25, taking $\sigma_f = 1600$ MPa, E = 210 GPa for steel. The solution of these equations is given by the intersection of the two curves shown in the figure, which suggests a combination of length/width of L=83.5 mm and thickness of h=3.3 mm. This configuration may not have a large region of uniform stress, but as discussed in the introduction, this is not a requirement for biaxial deformation testing. The respective failure surface and buckling locus are shown in Figure 26, which depicts the useable loading path in compressive region if buckling is to be avoided.

5. Conclusions

The achievements at AMRL to date for the design and commissioning of a biaxial test system are as follows.

1. The biaxial test machine is now fully functional and is capable of running under both load and strain control conditions. The strain-control capability has been successfully implemented which now allows plastic deformation tests to be conducted. The control system is an improvement over the previous one and has overcome the main limitations in the test machine.

2. A number of biaxial tests have been completed under elastic and/or plastic loading condition, for 7050 al-alloy and D6AC steel. These results will be useful in validating the constitutive model currently being developed at AMRL.

3. The result from a closed form cyclic elastic/plastic stress strain relationship theory for uniaxial loading has been compared to an experimental result, and good agreement was observed. This theory was extended to multiaxial loading in the appendix, which may serve as an alternative to the incremental constitutive model. Good agreement with experimental results has been observed.

4. The original specimen design has been shown to be mostly unsuitable for plastic loading, especially for D6AC steel. Two critical problems with the specimens are; (a) the total load required to generate 10,000 micro strain in two directions will exceed the machine capacity (500 kN in either axis), and (b) the specimen would buckle at a compressive load of about 200 kN, a level which will easily be exceeded under cyclic loading due to the Baushinger effect (a compressive load of 200 kN would be required to unload the specimen to zero strain after being strained to 1%).

5. New specimen design requirements have been recommended for any future biaxial work, which eliminates the problems of specimen buckling and exceeding the machine load capacity.

6. Acknowledgements

The authors wish to thank Dr G. Jost and Dr J. Finney for their helpful advice.

7. References

1. Finney, J. M. and Beaver, P. W. "The need for biaxial fatigue testing at A. R. L.", Structures Technical memorandum 380, AR-003-028, 1984.
2. Rees, D. "Continuation of the biaxial test program", Minute, File B2.129/1, 26/10/93.
3. He, D. T., Williams, J. F., Rees, D. and Jones, R. "A specimen for experimentally investigating the biaxial behaviour of a constitutive model", Internal report No. SM/2/92, Dept. of Mechanical and Manufacturing Engineering, University of Melbourne, 1992.
4. Brown, M. W. and Miller, K. J. "Mode I fatigue crack growth under biaxial stress at room and elevated temperature", *Multiaxial Fatigue, ASTM STP 853*, K. J. Miller and M. W. Brown, Eds., American Society for Testing and materials, Philadelphia, pp. 135-152, 1985.
5. Searl, A. and Paul, J. "Characterisation of D6AC steel using a unified constitutive model", DSTO Research Report, Airframes and Engines Division, AMRL, 1996 (In publication).
6. Damage Tolerant Design Handbook, Metals and Ceramics Information Centre, Battelle Columbus Laboratories, MCiC-HB-01R, 1983.
7. Wang, C. H. and Brown, M. W. "Experimental and theoretical study of the deformation behaviour of En15R steel under multiaxial loading", *Multiaxial Plasticity*, Mecamat, Paris, pp. 256-277, 1992.
8. Wang, C. H. and Brown, M. W. "A study of the deformation behaviour under multiaxial loading", *European Journal of Mechanics, A/Solids*, **13**, pp. 175-188, 1994.
9. Timoshenko, S. P. and Woinowsky-Krieger, 'Theory of plates and shells', McGraw-Hill, 1959.
10. Young, W. C. "Roark's Formulas for Stress and Strains", 6th Edition, McGraw-Hill, New York, p.685, 1989.
11. Wang, C. H. and Brown, M. W. "On plastic deformation and fatigue under multiaxial loading", Nuclear Engineering and Design, Vol. 162, pp. 75-84, 1995.

Appendix: Deformation theory for cyclic plasticity

To facilitate the following analysis, we denote the horizontal and vertical loads as P_x and P_y, the respective stresses and strains as $\sigma_x, \sigma_y, \varepsilon_x, \varepsilon_y$. If the loading is proportional, the principal plastic strain orientation remains the same as the principal stress orientation,

$$\varepsilon_{ij}^p = \lambda s_{ij} \tag{A1}$$

where s_{ij} are the deviatoric stress tensor and λ is a proportion factor, which is positive during loading and zero during elastic unloading. Define $\bar{\varepsilon}^p = \sqrt{2/3\varepsilon_{ij}^p \varepsilon_{ij}^p}$ and $\bar{\sigma} = \sqrt{3/2 s_{ij} s_{ij}}$, we have $\lambda = 3\bar{\varepsilon}^p / 2\bar{\sigma}$. Here $\varepsilon_{ij}^{'} (= \varepsilon_{ij} - \varepsilon_{mm}/3\delta_{ij})$ is the deviatoric strain tensor and $s_{ij} = \sigma_{ij} - \sigma_{mm}/3\delta_{ij}$ is the deviatoric stress tensor. Therefore the biaxial stress-strain relationship for proportional loading can be expressed as the following via Hencky's equations,

$$\varepsilon_{ij} = \frac{(1+\nu')\bar{\varepsilon}}{\bar{\sigma}} s_{ij} + (1-2\nu)\frac{\sigma_{mm}}{3E}\delta_{ij} \tag{A2}$$

where ν' is the effective Poisson's ratio,

$$\nu' = 0.5 - (0.5-\nu)\frac{\bar{\sigma}}{E\bar{\varepsilon}} \tag{A3}$$

and the equivalent stress and strain are given by

$$\bar{\varepsilon} = \frac{1}{1+\nu'}\sqrt{\frac{3}{2}\varepsilon_{ij}^{'}\varepsilon_{ij}^{'}} \tag{A4}$$

where $\varepsilon_{ij}^{'} (= \varepsilon_{ij} - \varepsilon_{mm}/3\delta_{ij})$ are the deviatoric strain tensors and

$$\bar{\sigma} = \sqrt{\frac{3}{2} s_{ij} s_{ij}} \tag{A5}$$

The relationship between $\bar{\sigma}$ and $\bar{\varepsilon}$ is given by the uniaxial stress-strain curve, e.g. a Ramberg-Osgood relationship

$$\bar{\varepsilon} = f(\bar{\sigma}) = \frac{\bar{\sigma}}{E} + \left(\frac{\bar{\sigma}}{K}\right)^{1/n} \tag{A6}$$

For a given strain state, an iteration is required to obtain the correct value of the Poisson's ratio,

$$\nu' = 0.5 - (0.5 - \nu)\frac{f^{-1}(\sqrt{3/2\varepsilon_{ij}\varepsilon_{ij}}/(1+\nu'))}{E\sqrt{3/2\varepsilon_{ij}\varepsilon_{ij}}/(1+\nu')} \qquad \text{(A7)}$$

An inverse version of equation (A7) for calculating stress components once the strain components are known is

$$\sigma_{ij} = \frac{\bar{\sigma}}{(1+\nu')\bar{\varepsilon}}\varepsilon_{ij} + (\frac{E}{1-2\nu} - \frac{\bar{\sigma}}{(1+\nu')\bar{\varepsilon}})\frac{\varepsilon_{mm}}{3}\delta_{ij} \qquad \text{(A8)}$$

In the case of cyclic loading, the relative stress and strain concepts by Wang and Brown [7,8] can be used to predict the hysteresis strain hardening. Relative stresses and strains are defined as the differences between the instantaneous stresses and strains and their respective values at the previous turning point,

$$\varepsilon^*_{ij} = \varepsilon_{ij} - \varepsilon^R_{ij} \qquad \text{(A9)}$$

$$\sigma^*_{ij} = \sigma_{ij} - \sigma^R_{ij} \qquad \text{(A10)}$$

The equivalent relative stress and strain can also be defined similarly to equations (A14) and (A15), replacing the stress and strain tensors by the relative stress and strain tensors, respectively. In this case, Hencky's assumption is still valid, namely,

$$(\varepsilon^p_{ij})^* = \lambda^* s^*_{ij} \qquad \text{(A11)}$$

where

$$\lambda^* = \frac{3\bar{\varepsilon}^{*p}}{2\bar{\sigma}^*} \qquad \text{(A12)}$$

Equations (A7) to (A13) also hold for relative stresses and strains. Therefore the instantaneous stresses and strains are related through the following equation

$$\varepsilon_{ij} = \varepsilon^R_{ij} + \frac{(1+\nu^*)\bar{\varepsilon}^*}{\bar{\sigma}^*}s^*_{ij} + (1-2\nu)\frac{\sigma^*_{mm}}{3E}\delta_{ij} \qquad \text{(A13)}$$

Turning points are defined as the peak or trough of a loading sequence, which are invariably followed by an elastic unloading. For a proportional loading sequence, the range pair or rainflow counting methods can be used to identify the turning points. In

the case of quasi-proportional loading, however, a more general counting method [11] should be utilised to identify correct turning points.

To illustrate the present methodology, consider the example shown in Figure 22. The residual strains $\varepsilon_x^R = 2000\ \mu\varepsilon$ and $\varepsilon_y^R = -438\ \mu\varepsilon$, the corresponding initial stresses are $\sigma_x^R = -414$ MPa and $\sigma_y^R = 92$ MPa when the strains are zeroed. Since the residual strains were resulted from previous cyclic loading, the hysteresis hardening equations need to be used in the predictions, hence the stresses are given by,

$$\sigma_x = \frac{\bar{\sigma}^*}{[1-(\nu')^2]\bar{\varepsilon}^*}(1+\nu'\beta)(\varepsilon_x - \varepsilon_x^R) + \sigma_x^R \qquad \text{(A14)}$$

$$\sigma_y = \frac{\bar{\sigma}^*}{[1-(\nu')^2]\bar{\varepsilon}^*}(1+\frac{\nu'}{\beta})(\varepsilon_y - \varepsilon_y^R) + \sigma_y^R \qquad \text{(A15)}$$

where ν' is given by equation (A12), except that the equivalent stress and strain should be replaced by the equivalent relative stress and strain. Alternatively, the strains can be expressed in terms of stresses,

$$\varepsilon_x = \frac{\sigma_x^* - \nu'\sigma_y^*}{\bar{\sigma}^*/\bar{\varepsilon}^*} + \varepsilon_x^R \qquad \text{(A16)}$$

$$\varepsilon_y = \frac{\sigma_y^* - \nu'\sigma_x^*}{\bar{\sigma}^*/\bar{\varepsilon}^*} + \varepsilon_y^R \qquad \text{(A17)}$$

A computer program was written to perform the above calculation; and the predictions and experimental results are shown in Figure 22. It can be seen that the predicted response correlates well with the experimental data. The plastic strains would be over-estimated if the effect of loading history is ignored and this half cycle is considered as monotonic loading; a prediction is also shown in the figure.

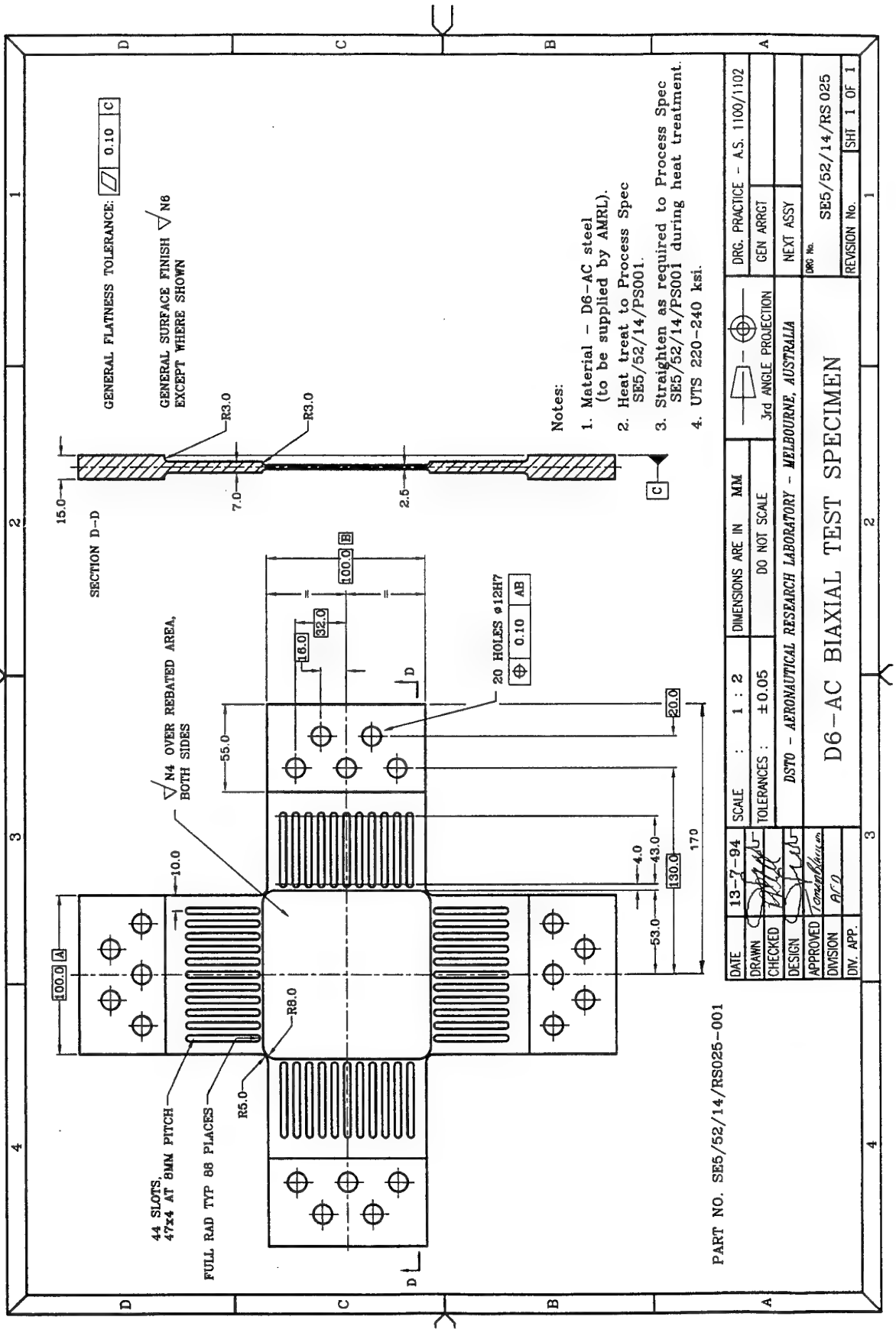

Fig.1 Geometry of cruciform specimen

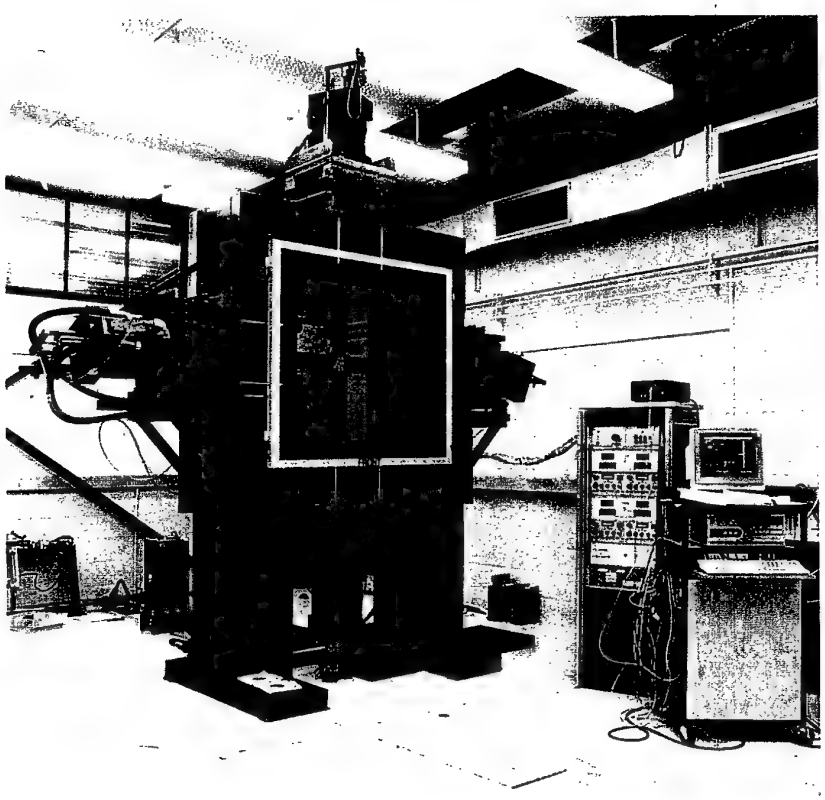

Fig. 2(a) Biaxial test machine

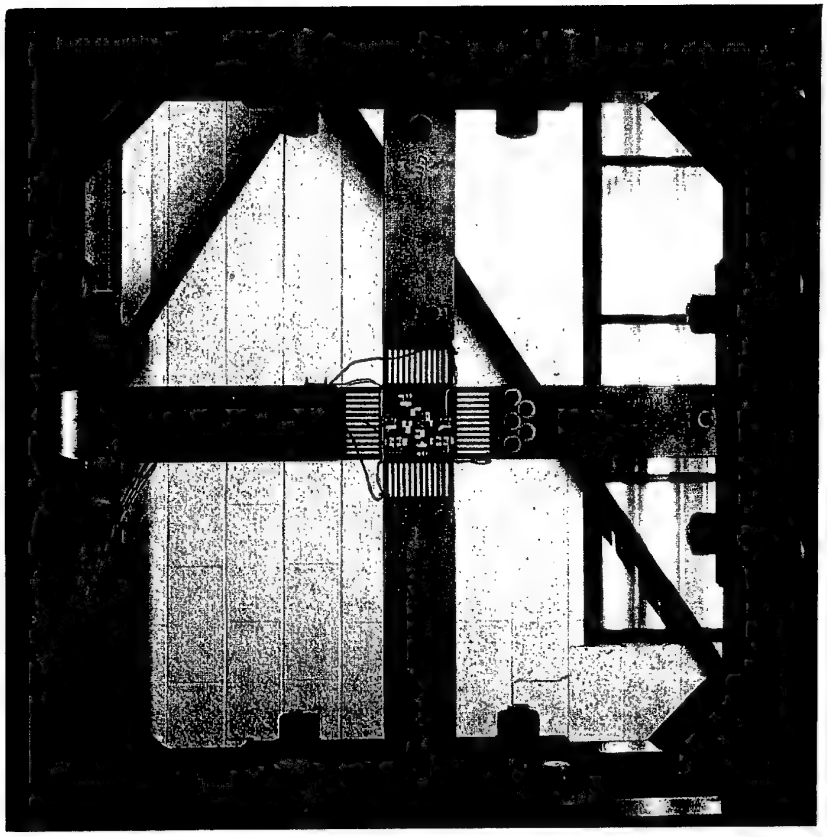

Fig. 2(b) Loading arrangement of specimen

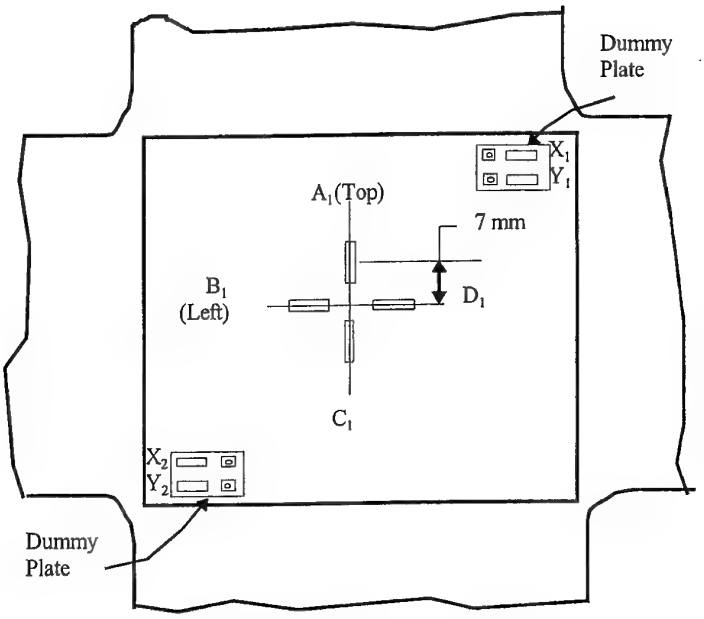

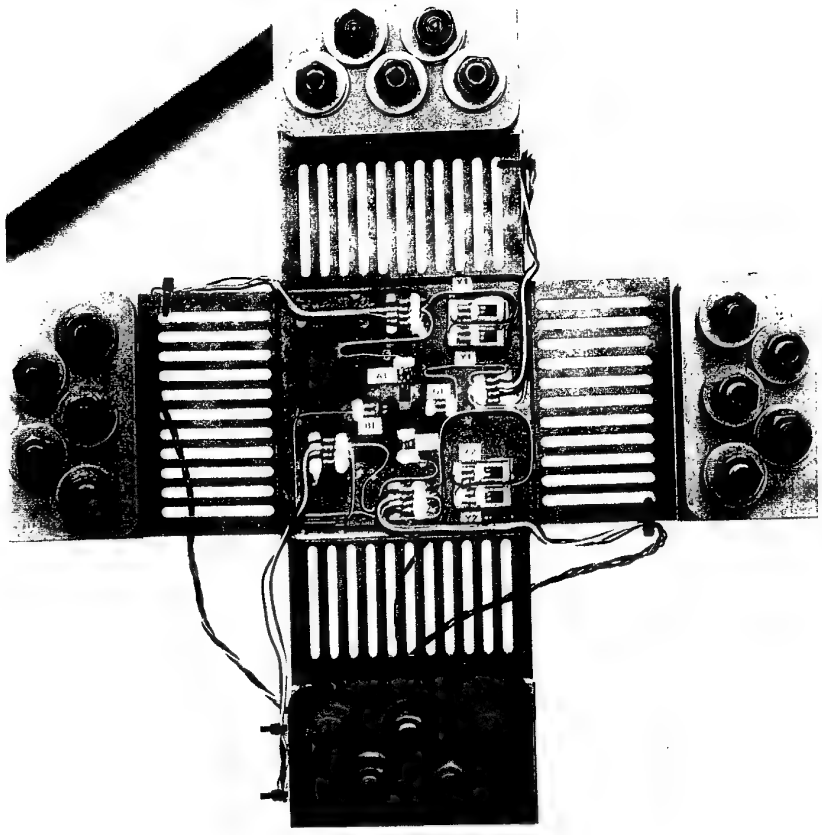

Fig.3 Strain gauge locations for control and monitoring of specimen strains.

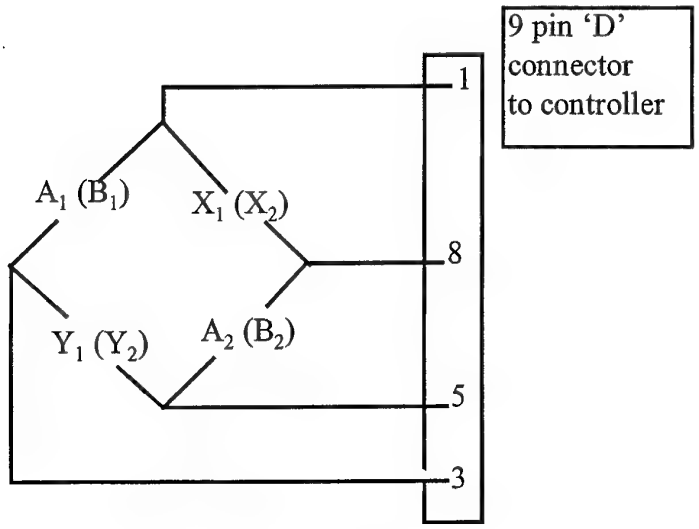

(a)

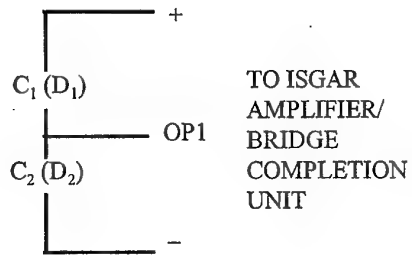

(b)

Fig.4 Circuit for the control and safety strain gauge bridges.
(Letters in brackets indicate strain gauges on back face of specimens.)

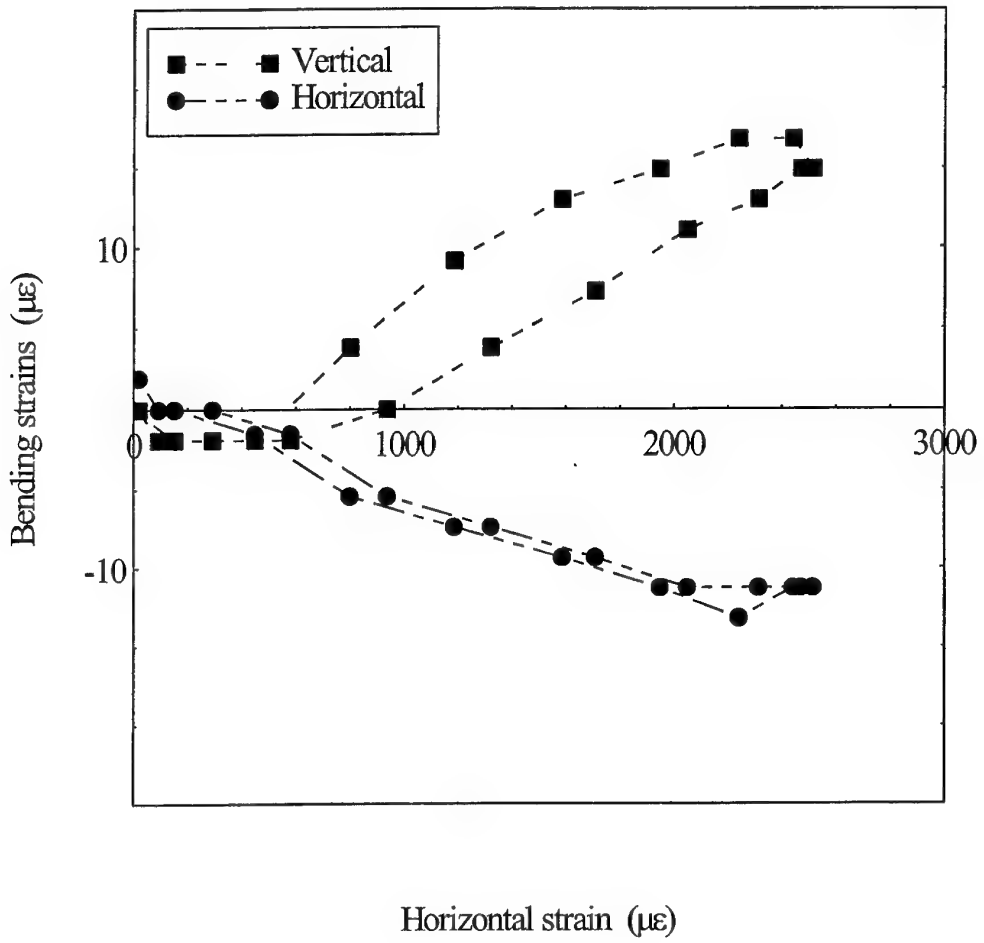

Fig. 5 Strain responses under horizontal loading only.

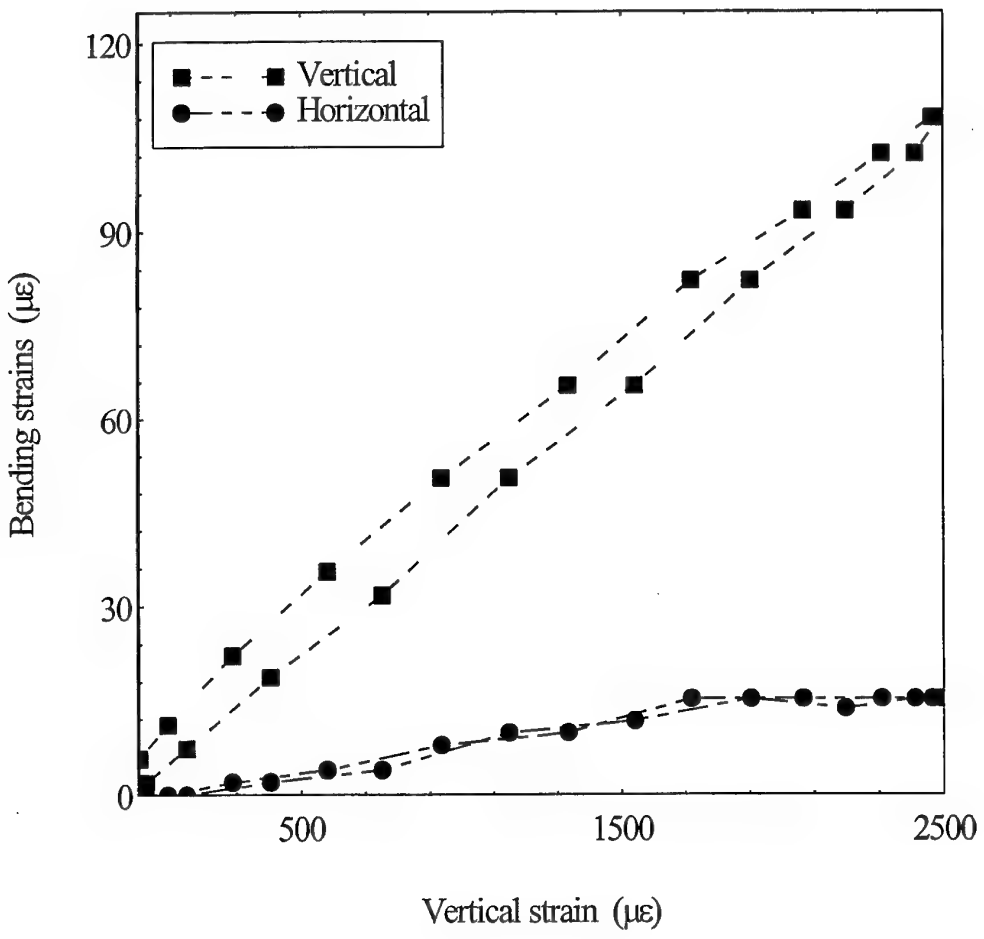

Fig.6 Strain responses under vertical loading only.

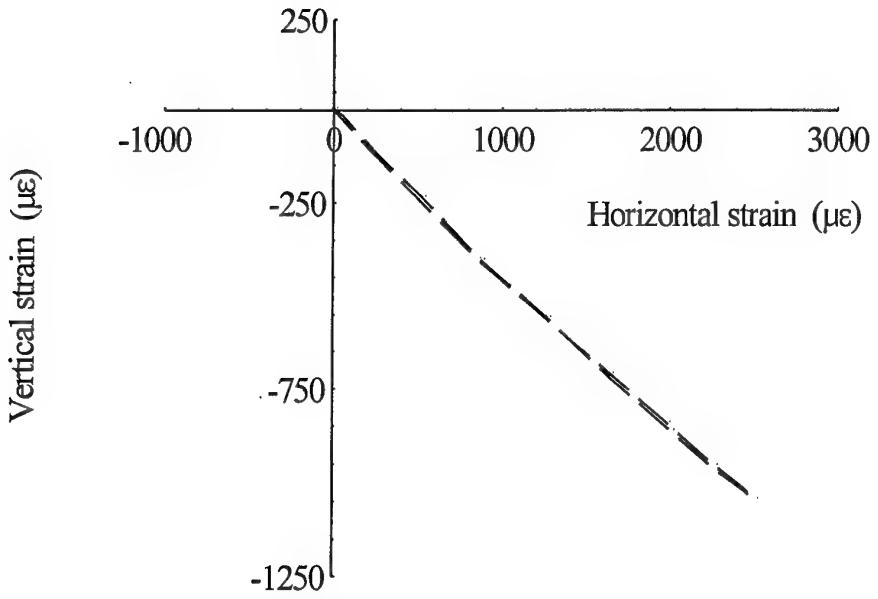

(a)

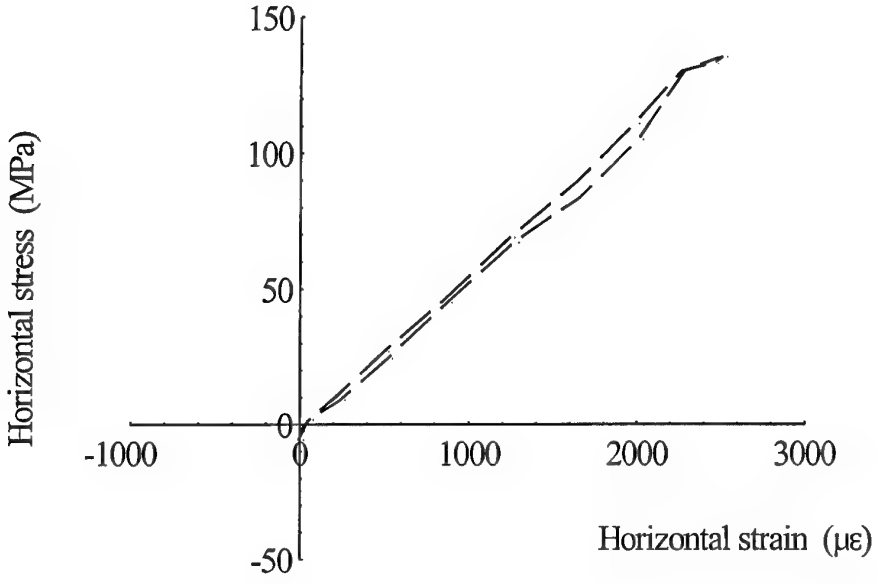

(b)

Fig.7 Deformation response of AL5083 under horizontal loading, $\beta = 0.3$.

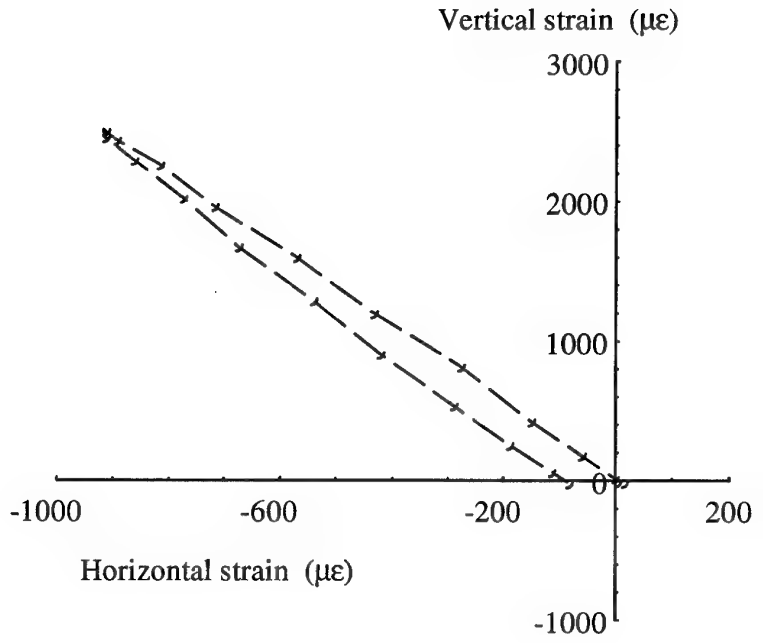

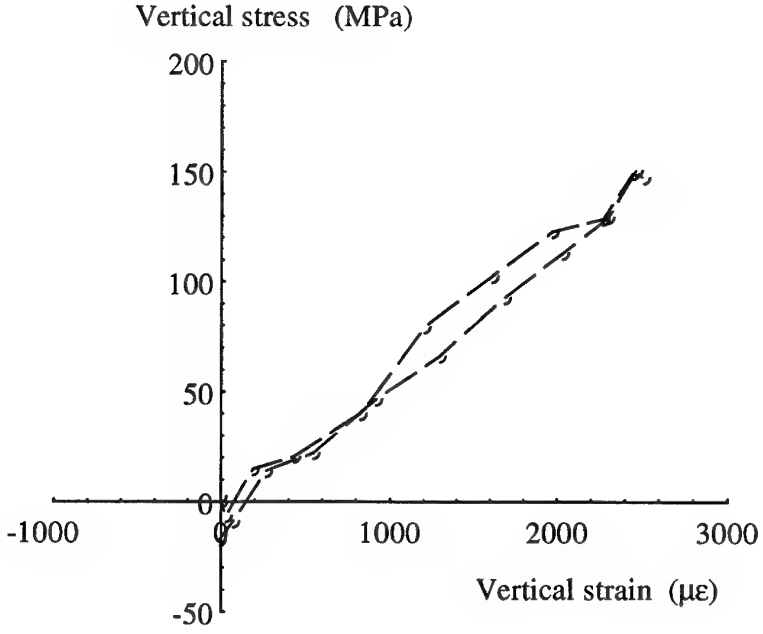

Fig.8 Deformation response of AL5083 under vertical loading, $\beta = -3.3$.

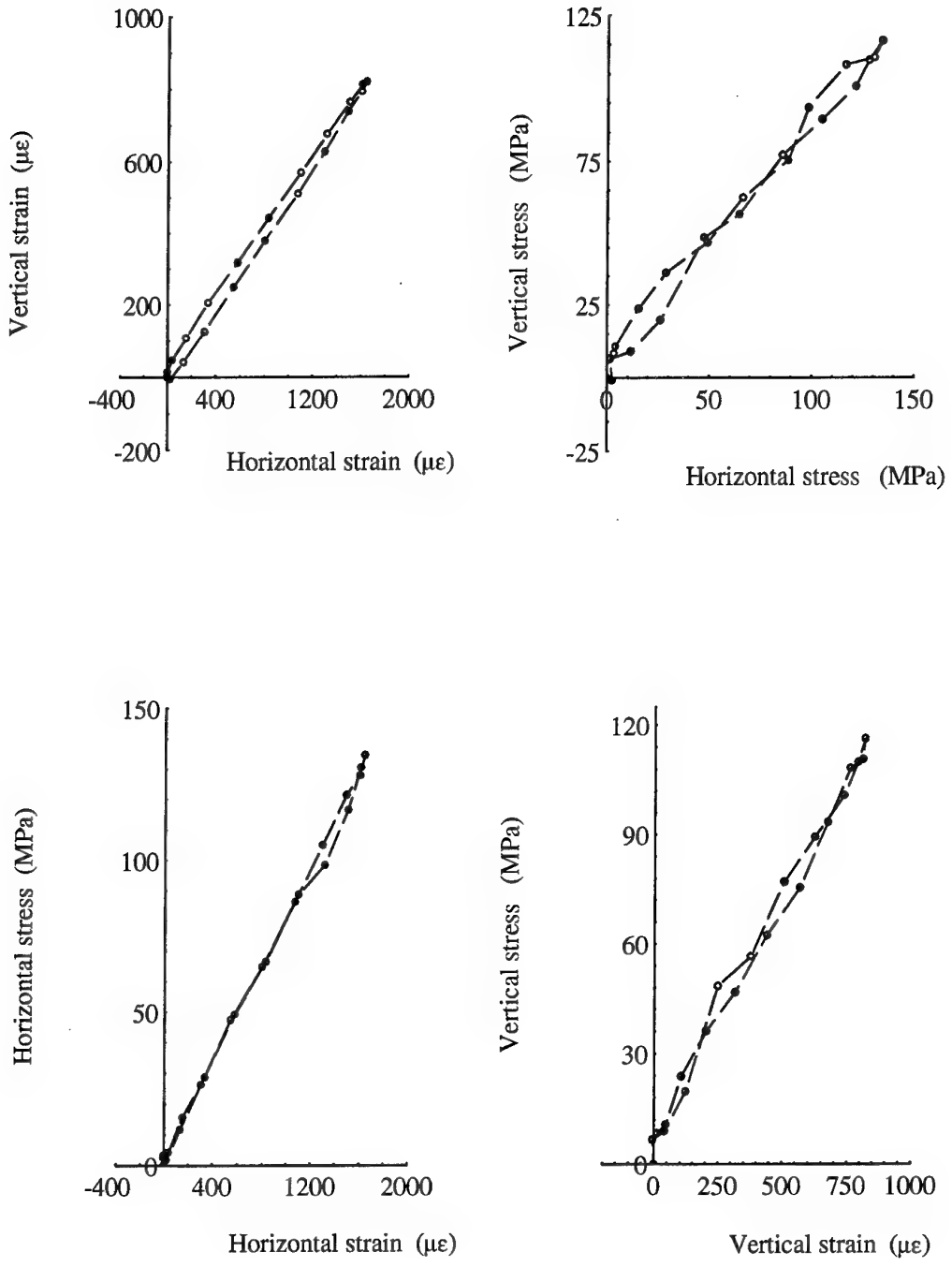

Fig.9 Deformation response of AL5083 under biaxial loading , $\beta = 0.5$.

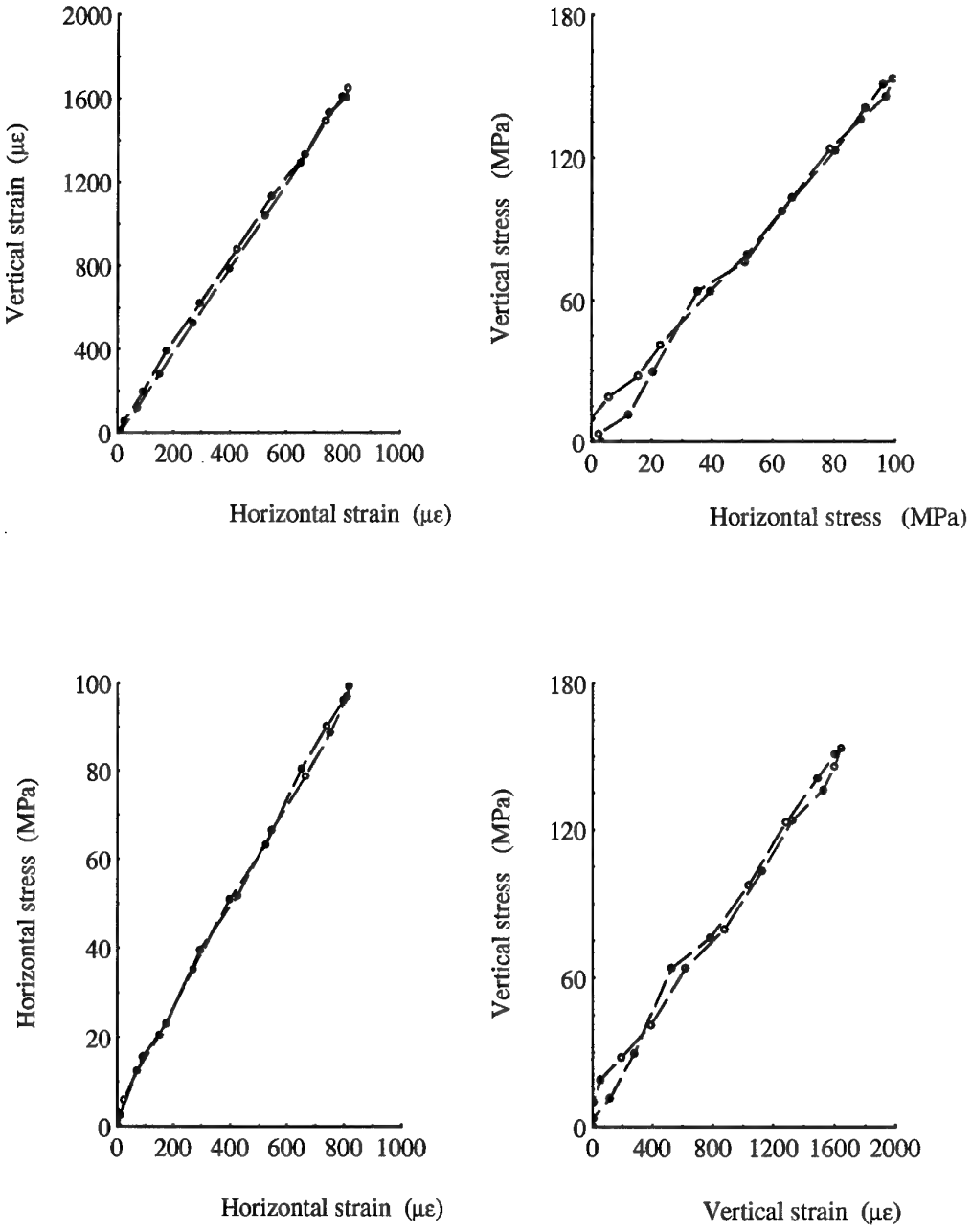

Fig.10 Deformation response of AL5083 under biaxial loading, $\beta = 2$.

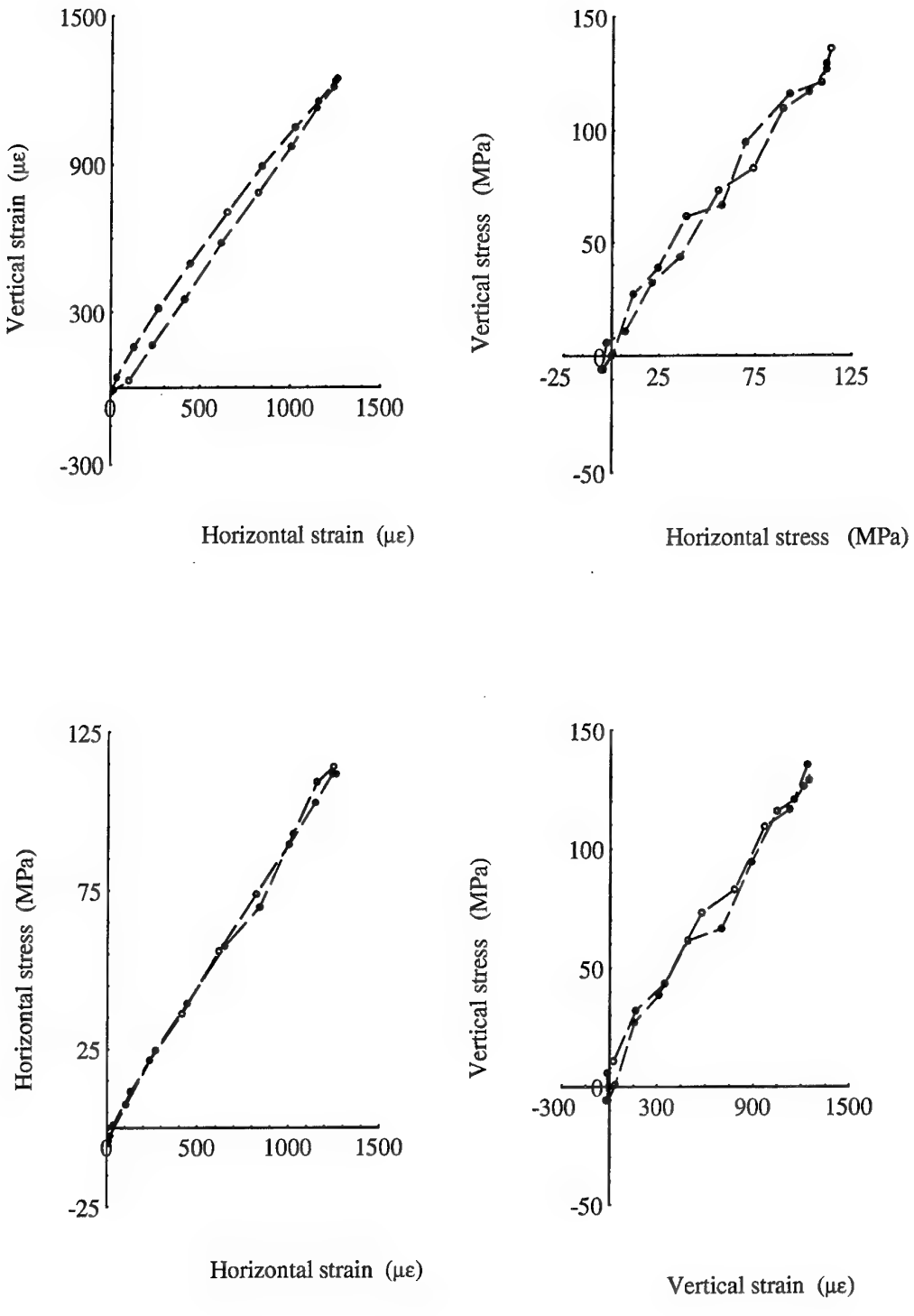

Fig.11 Deformation response of AL5083 under equi-biaxial loading, $\beta = 1$.

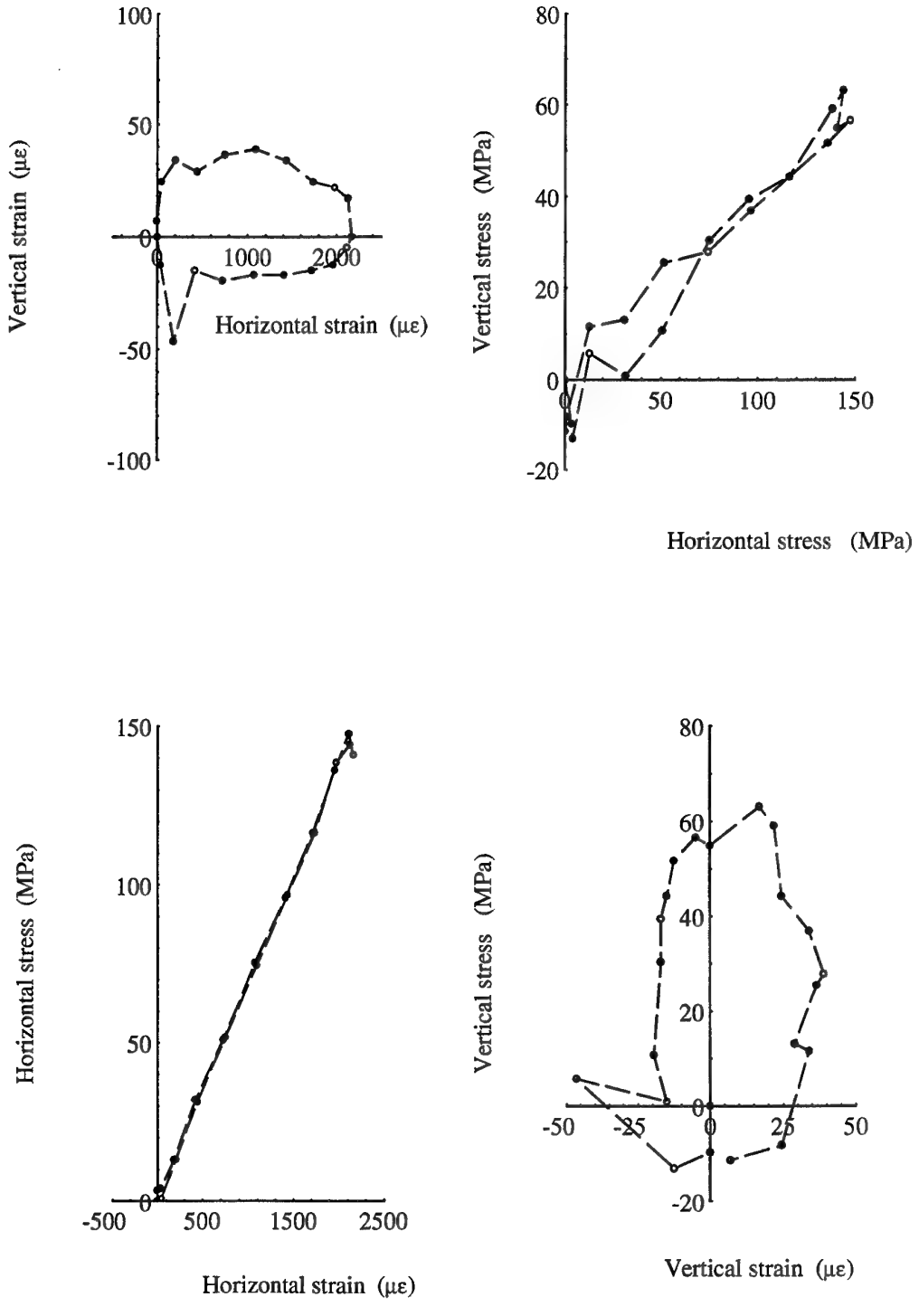

Fig.12 Deformation response of AL5083 under biaxial loading, $\beta = 0$.

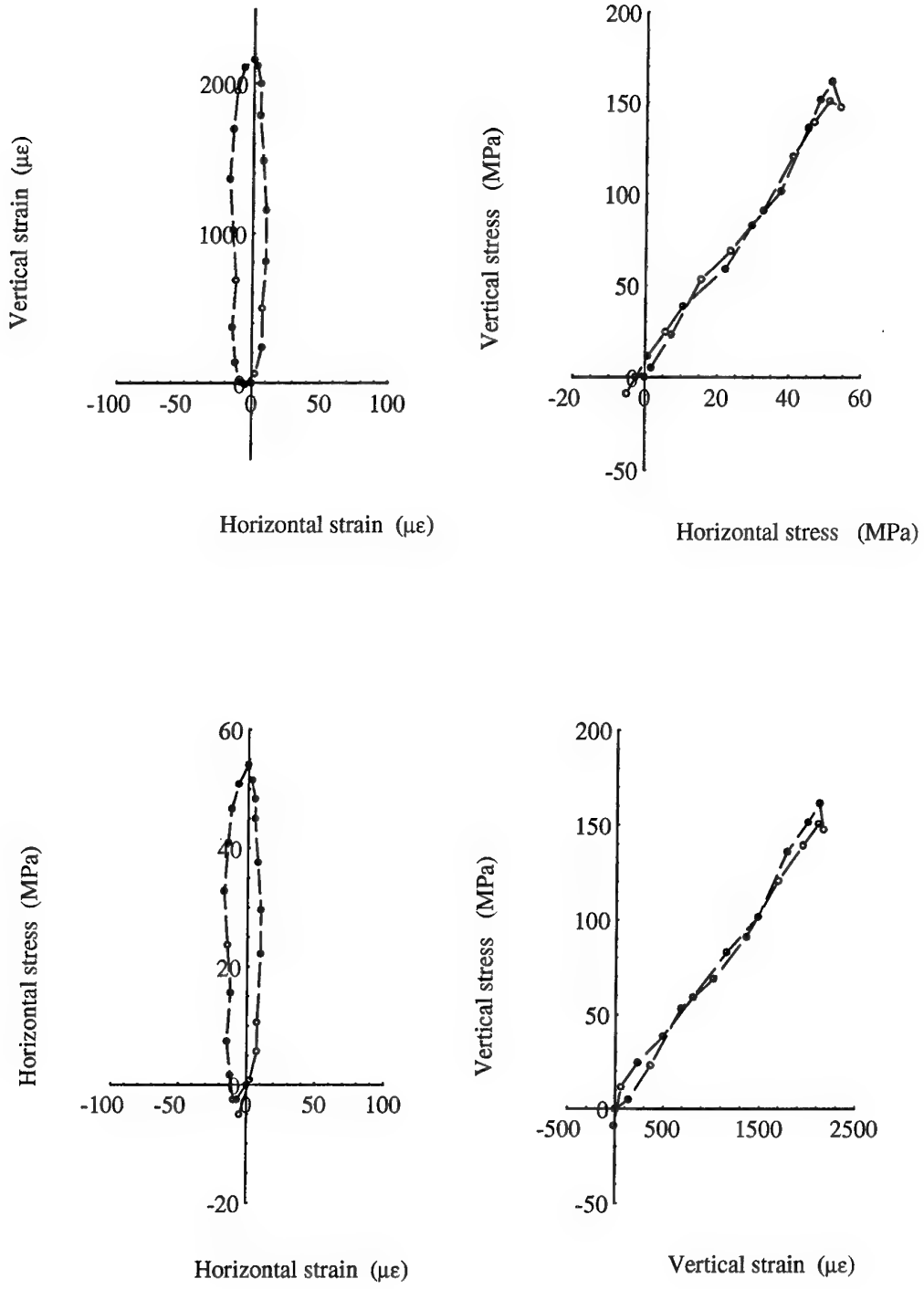

Fig.13 Deformation response of AL5083 under plane strain , $\beta = \infty$.

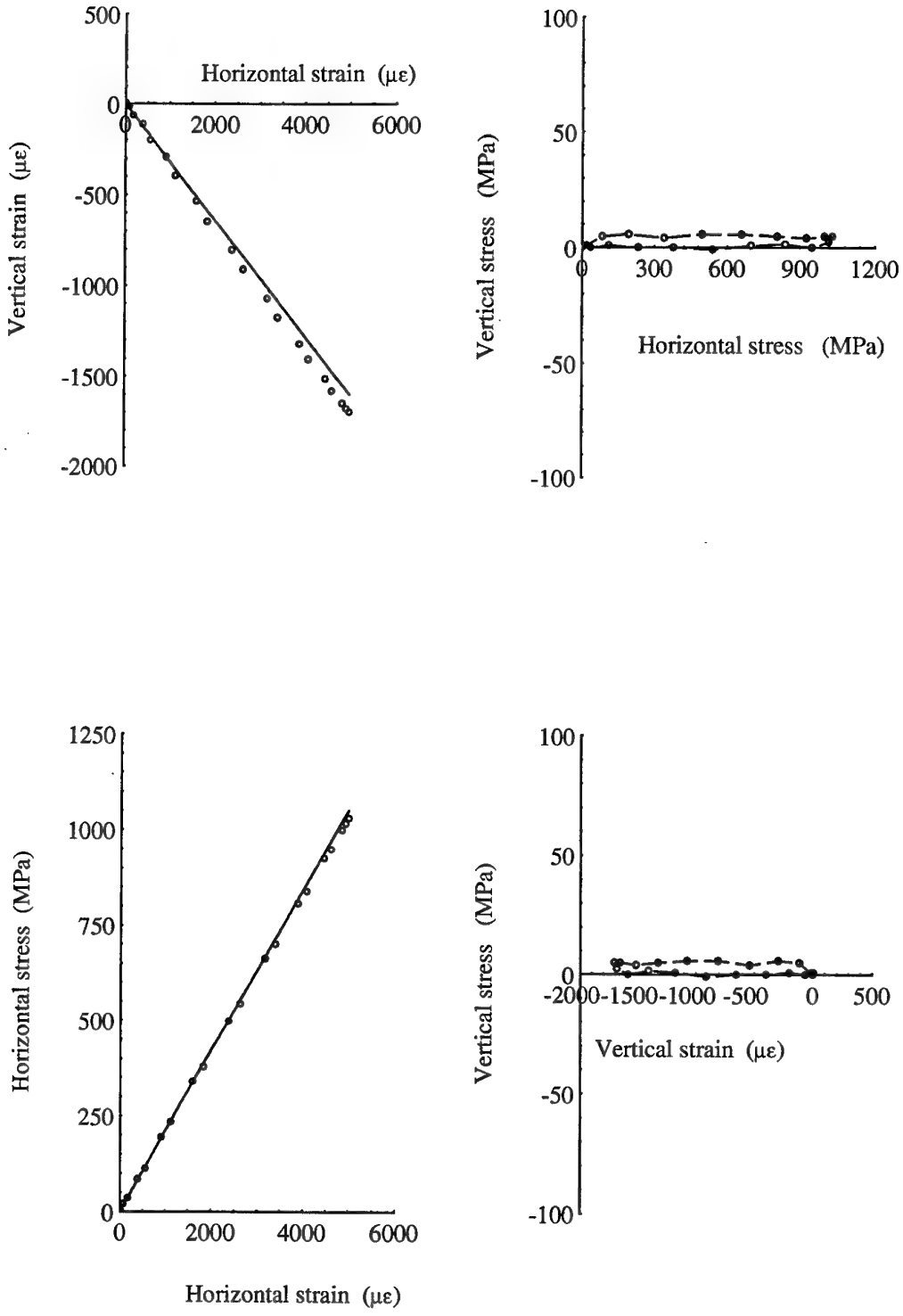

Fig.14 Deformation response of D6AC under horizontal loading, $\beta = -0.33$.

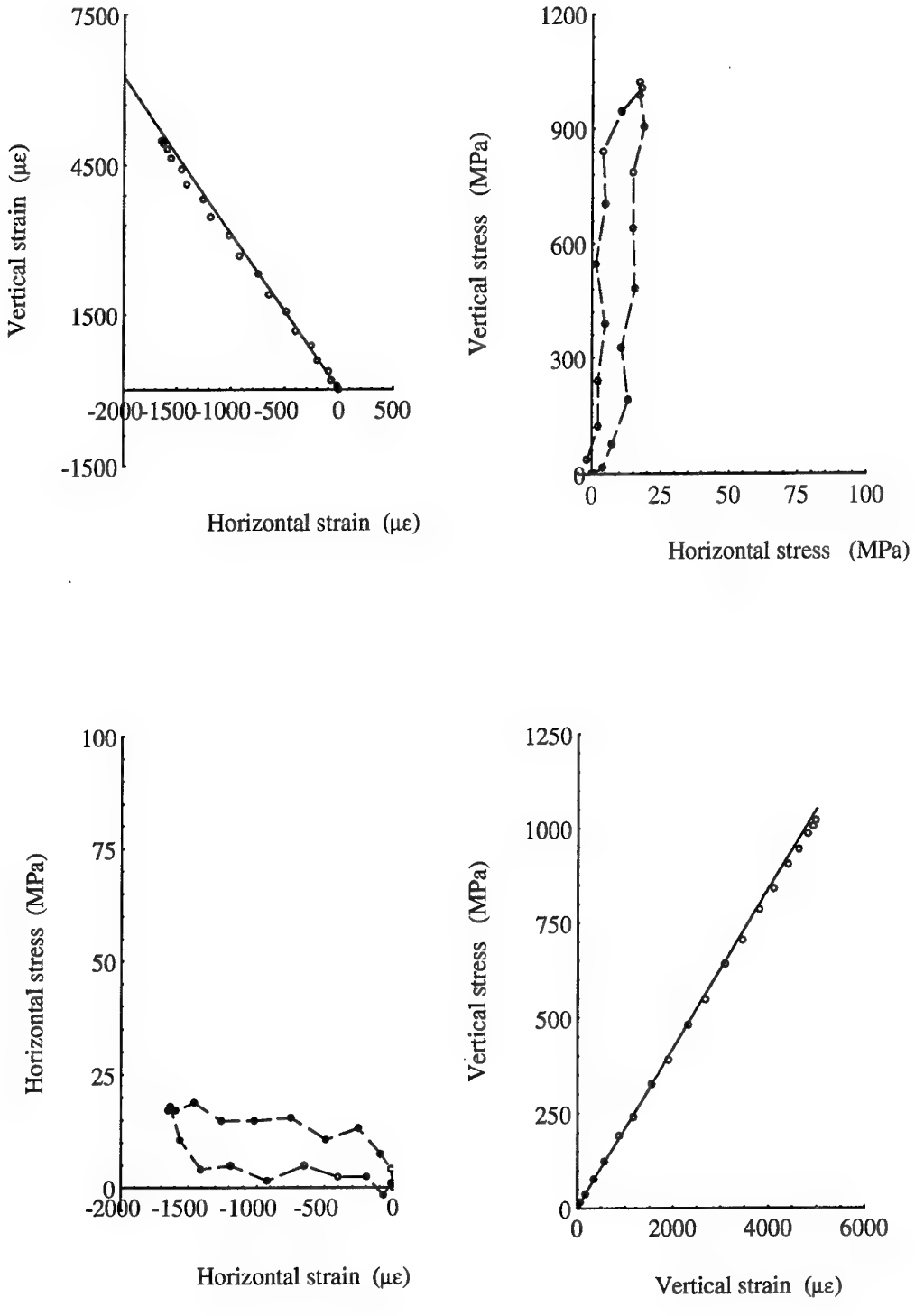

Fig.15 Deformation response of D6AC under vertical loading, $\beta = -3.0$.

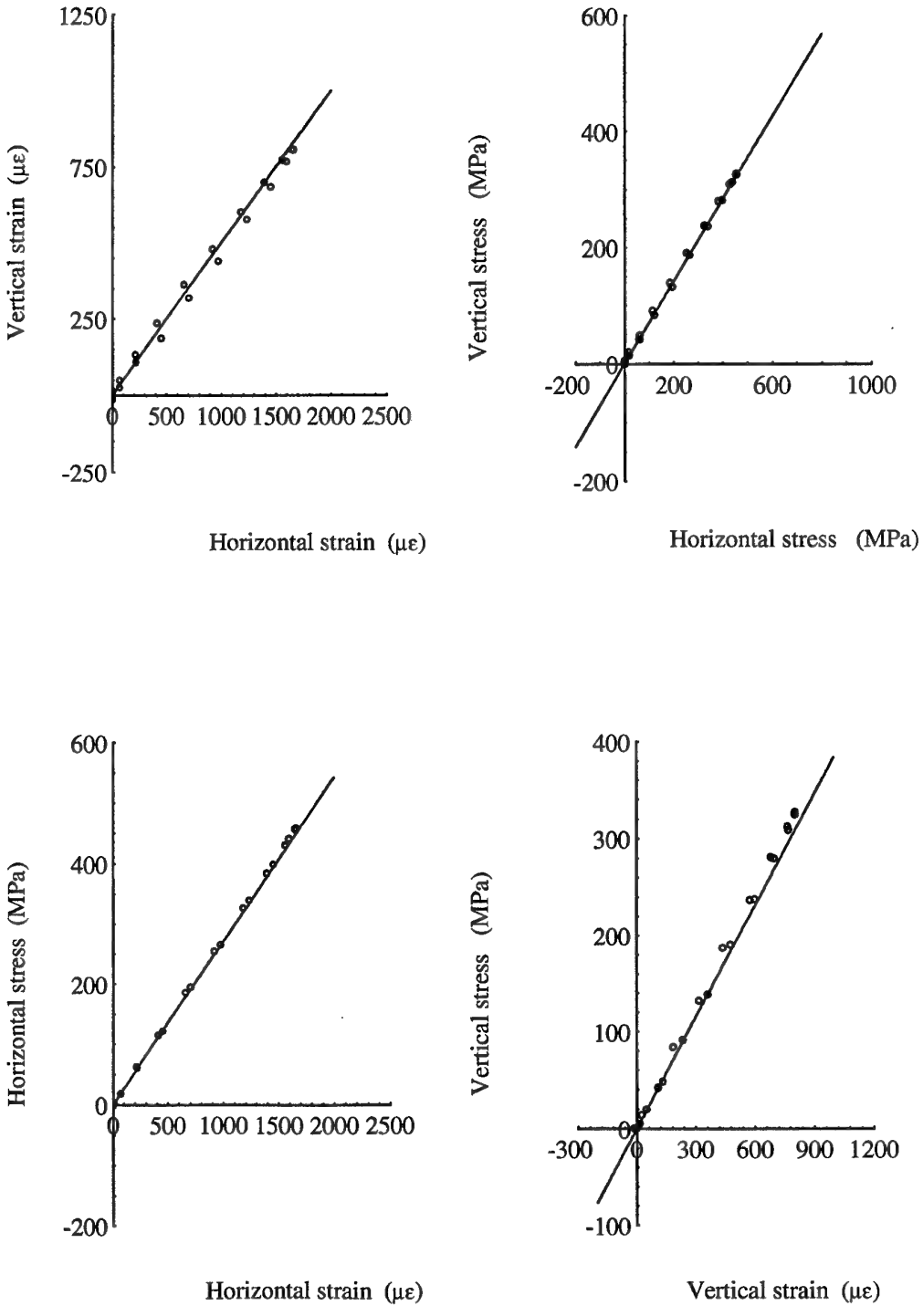

Fig.16 Deformation response of D6AC under biaxial loading, $\beta = 0.5$.

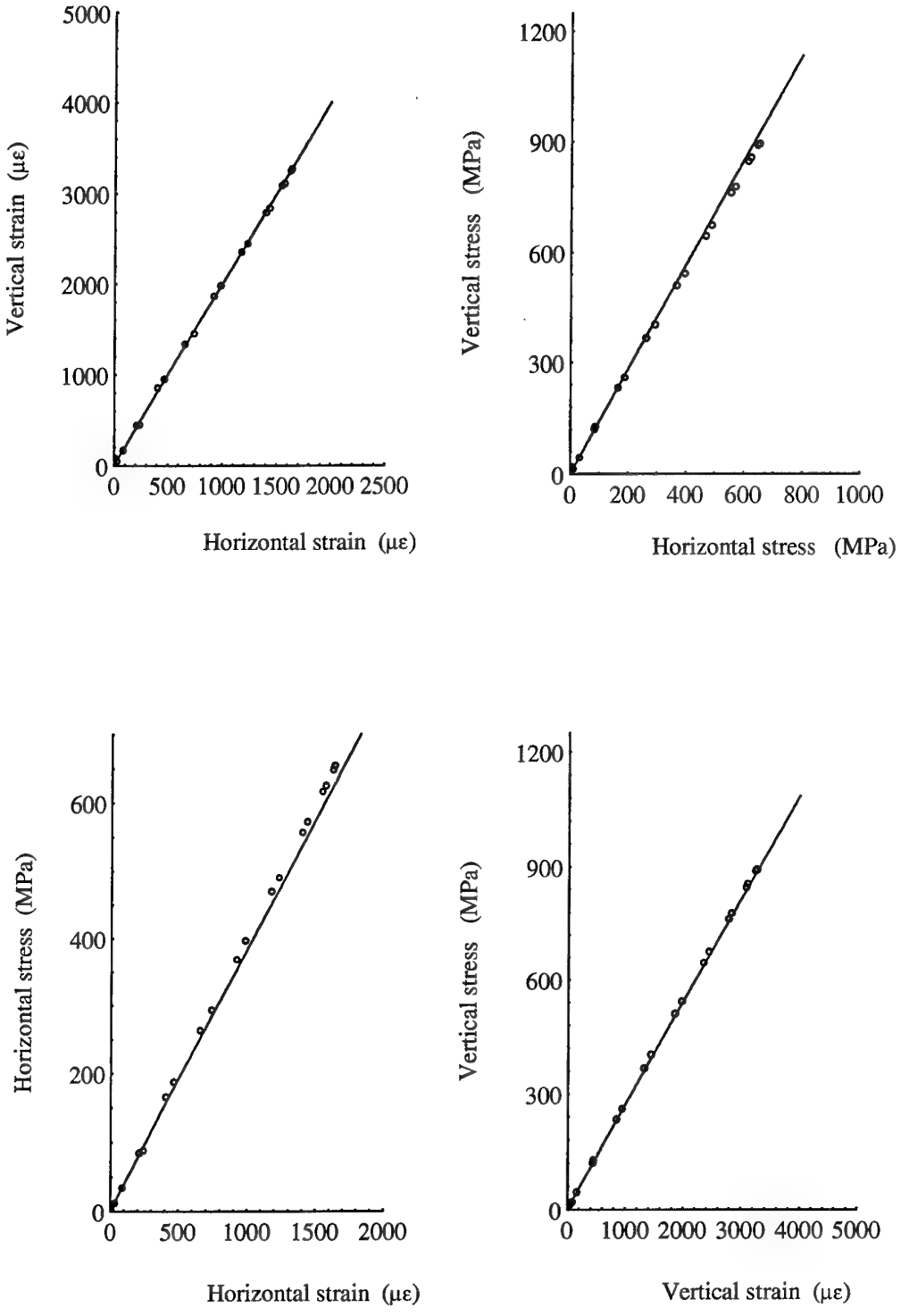

Fig.17 Deformation response of D6AC under biaxial loading, $\beta = 2$.

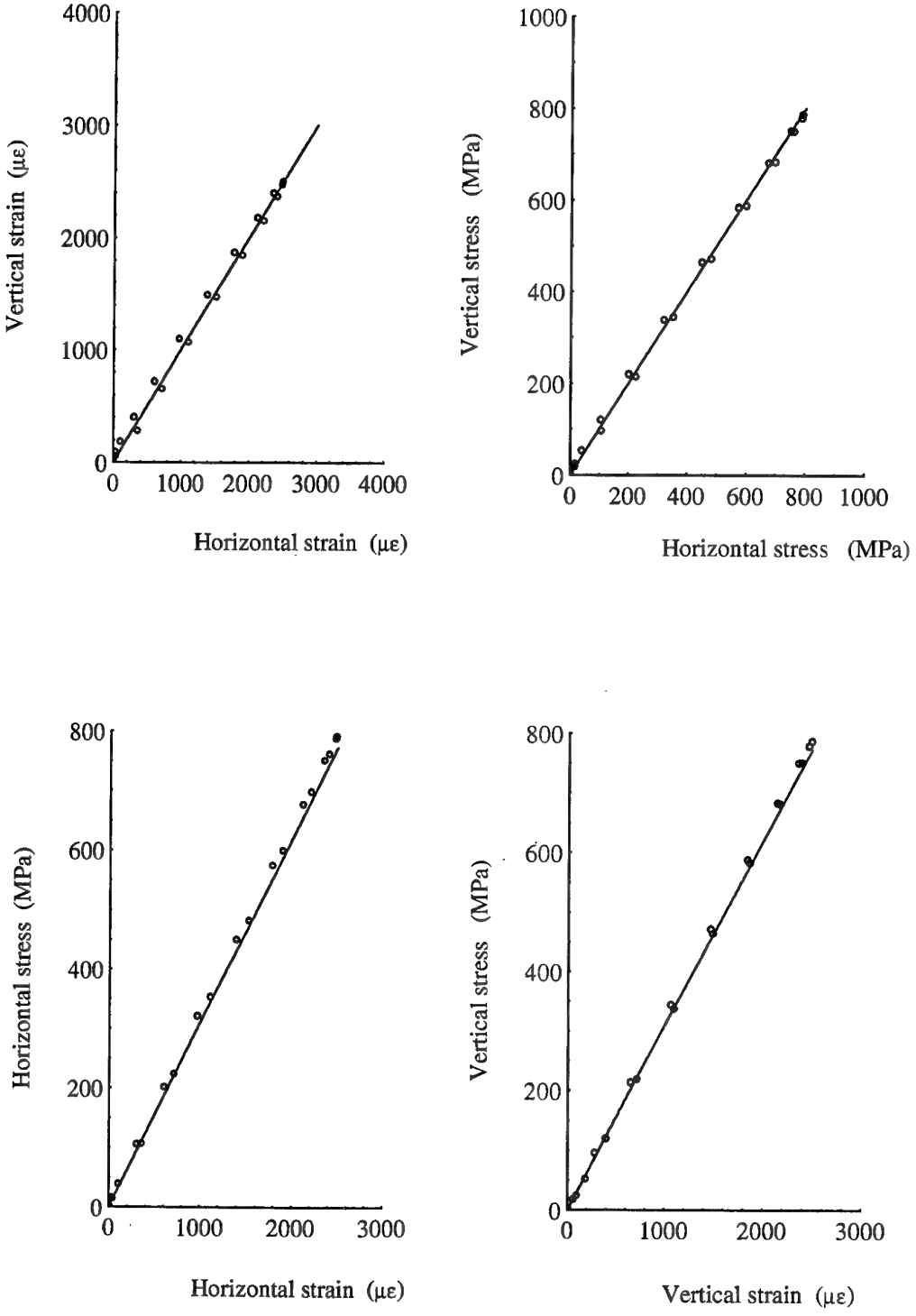

Fig.18 Deformation response of D6AC under equibiaxial loading, $\beta = 1$.

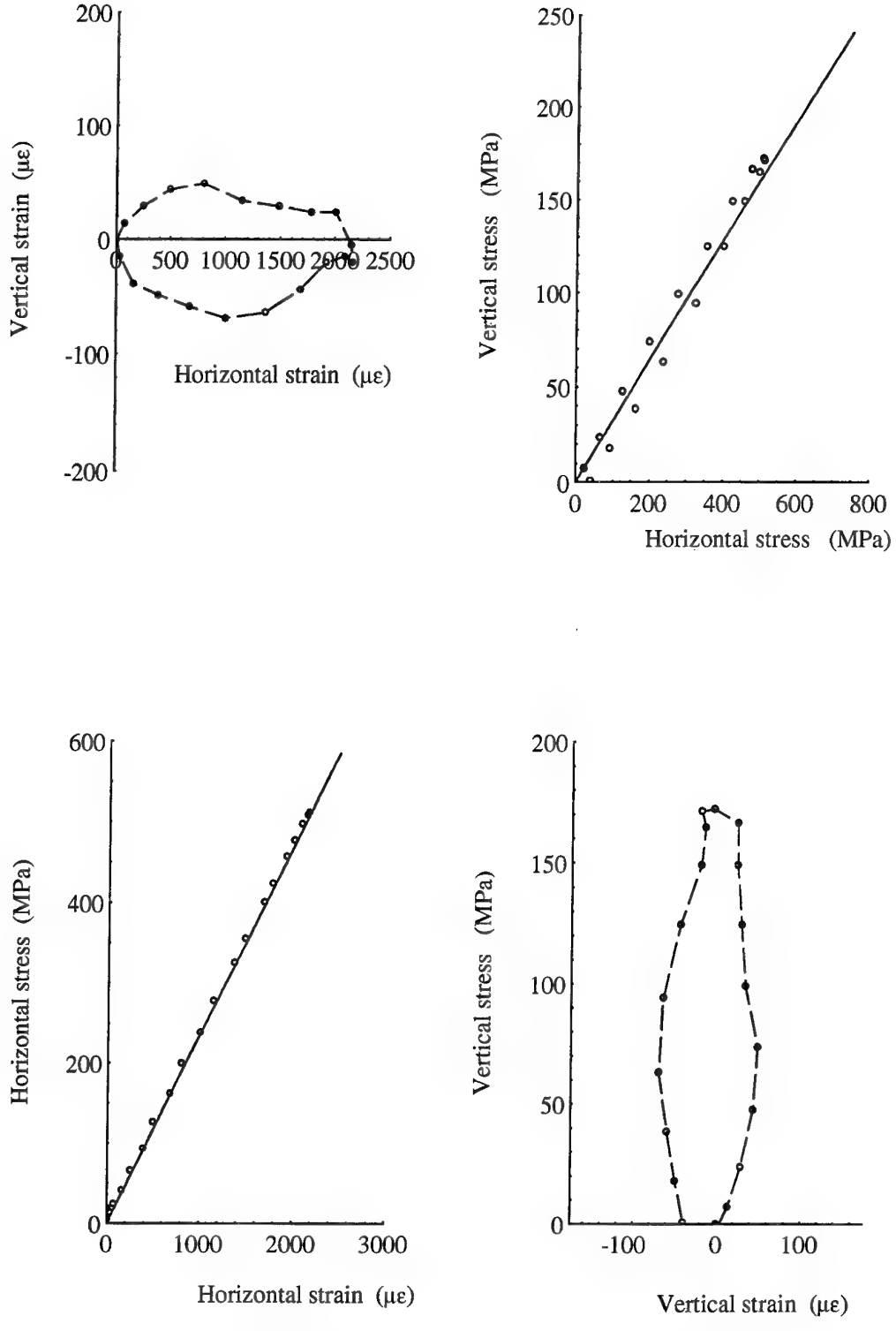

Fig.19 Deformation response of D6AC under plane strain condition, $\beta = 0$.

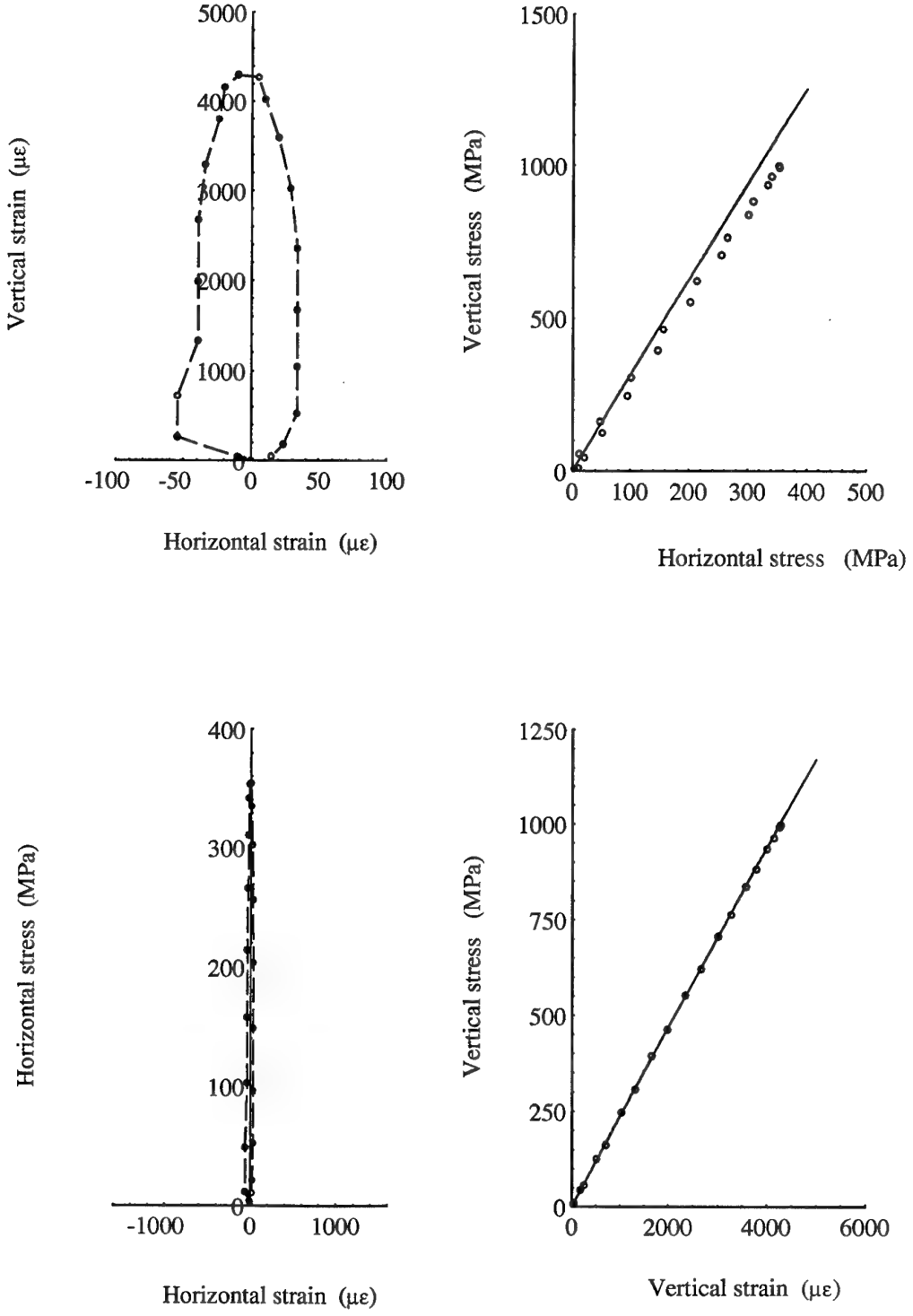

Fig.20 Deformation response of D6AC under plane strain condition, $\beta = \infty$.

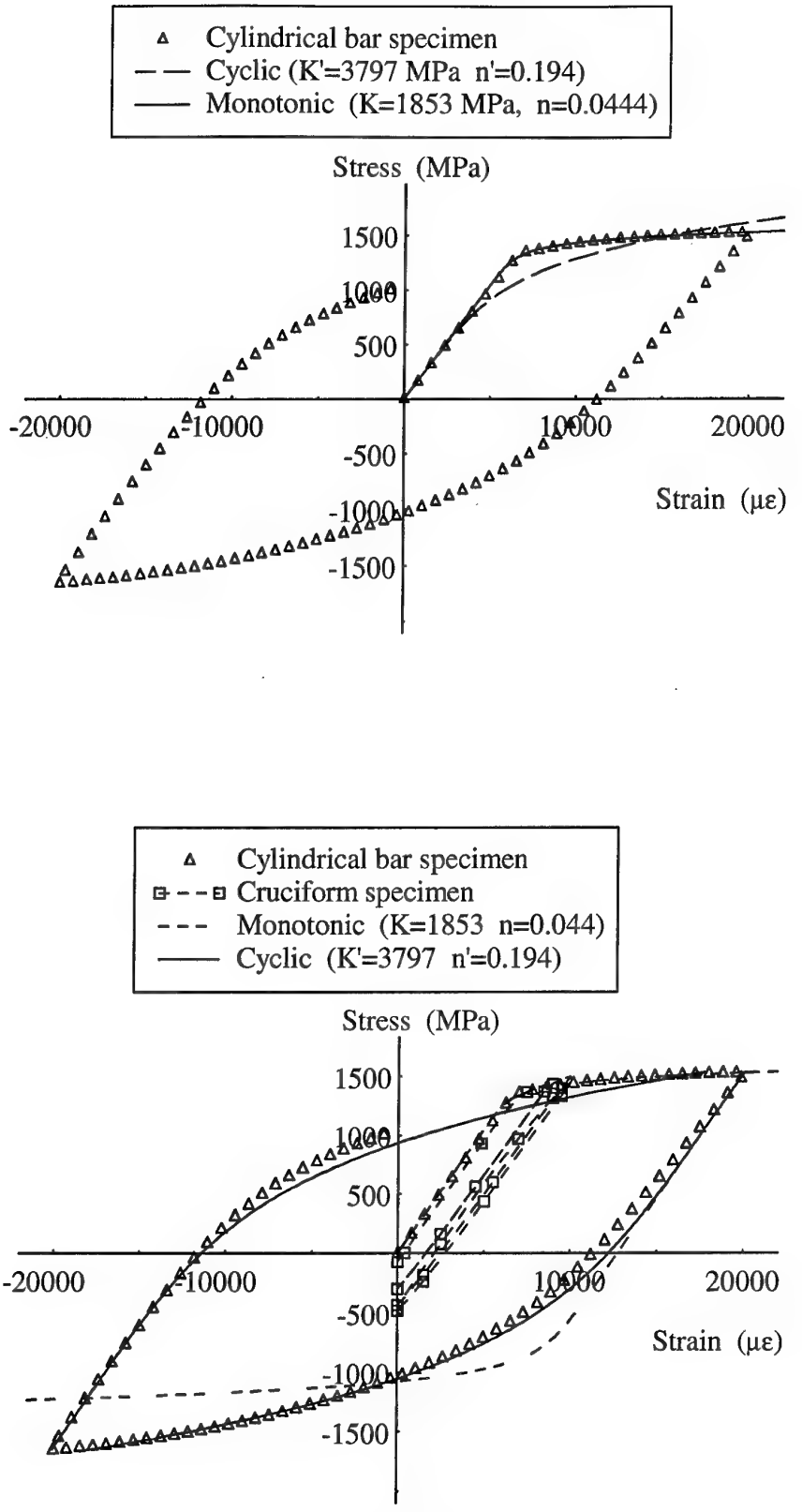

Fig.21 Monotonic and cyclic stress-strain response of D6AC steel..

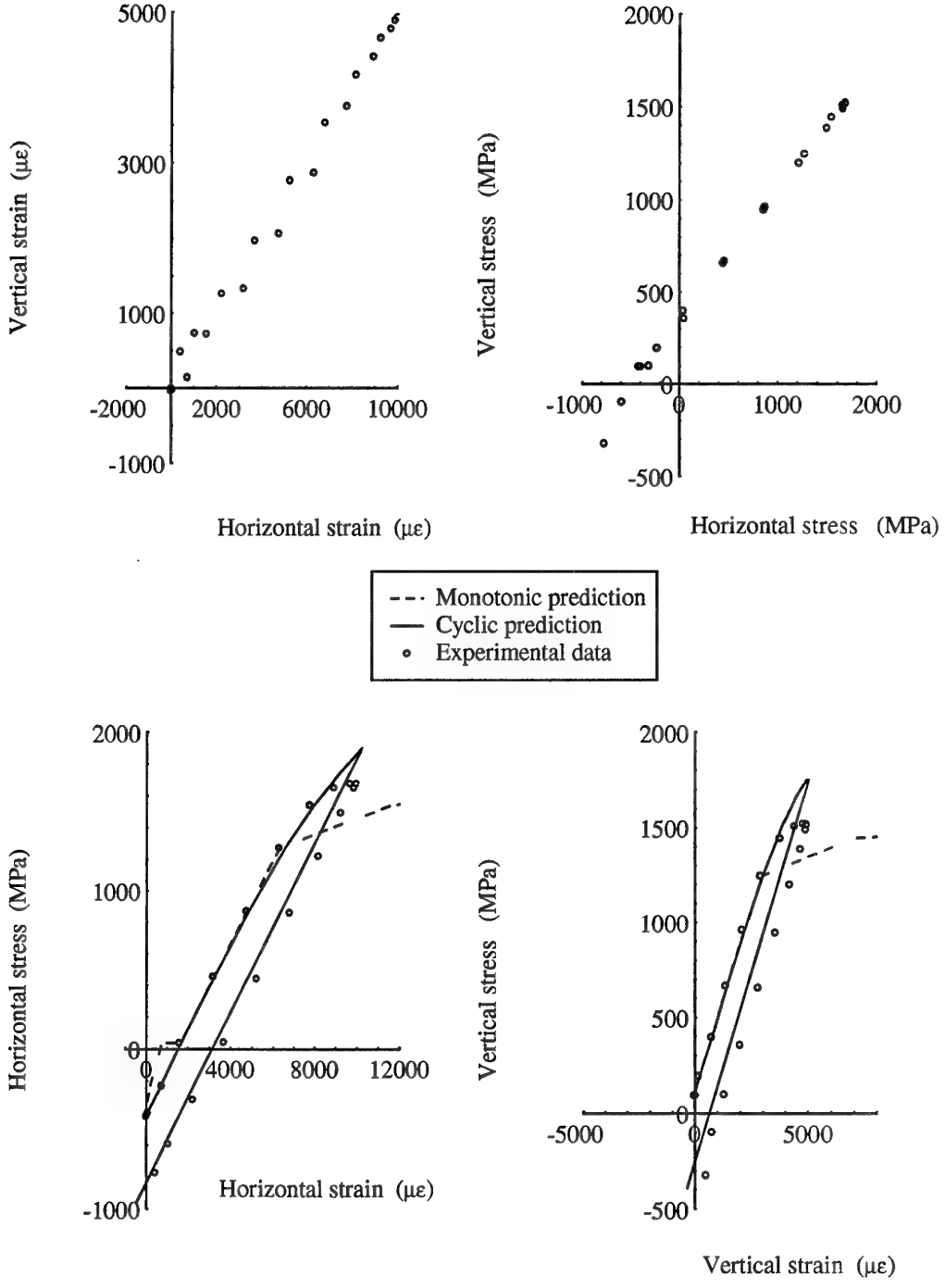

Fig.22 Deformation response of D6AC under proportional loading , $\beta = 0.5$.

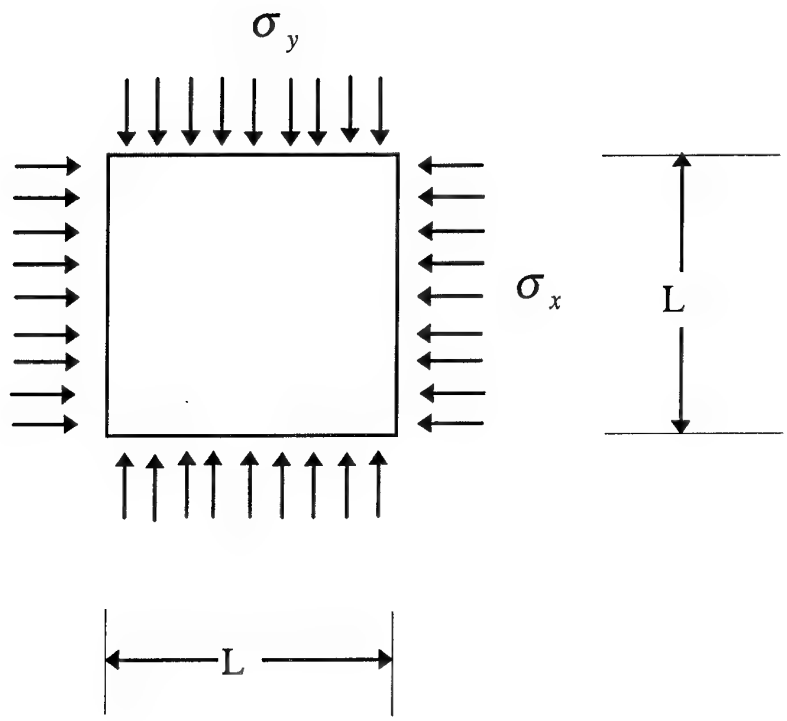

Fig.23 A square plate under biaxial loading.

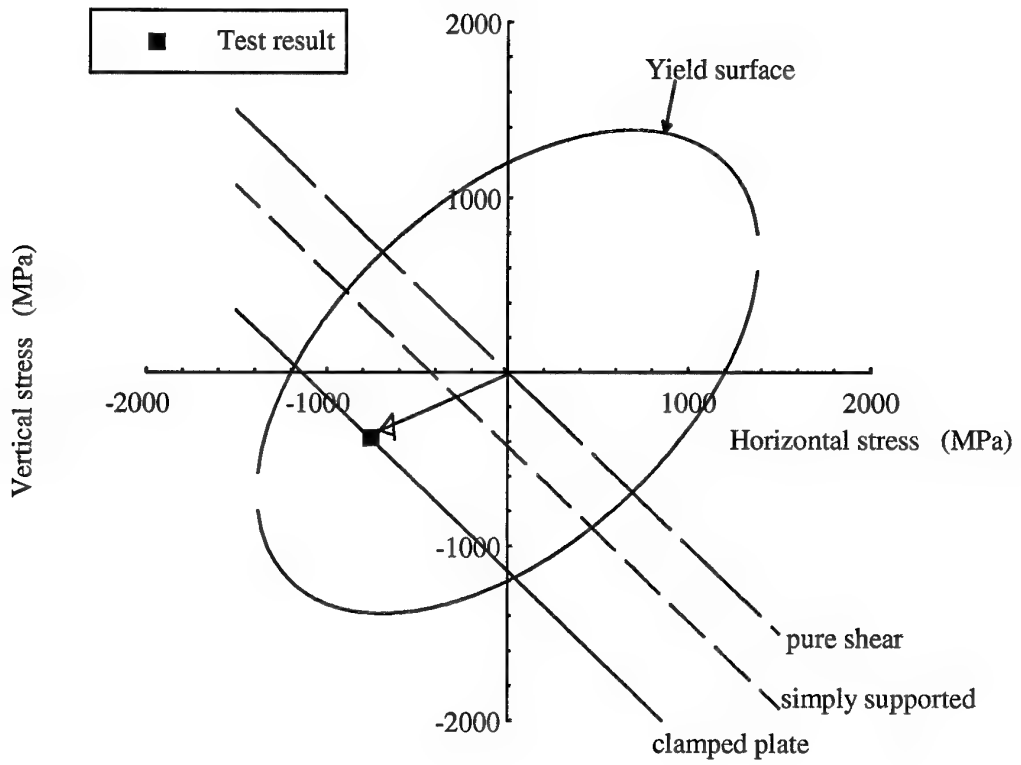

Fig.24 Yielding and buckling loci for the cruciform specimen.

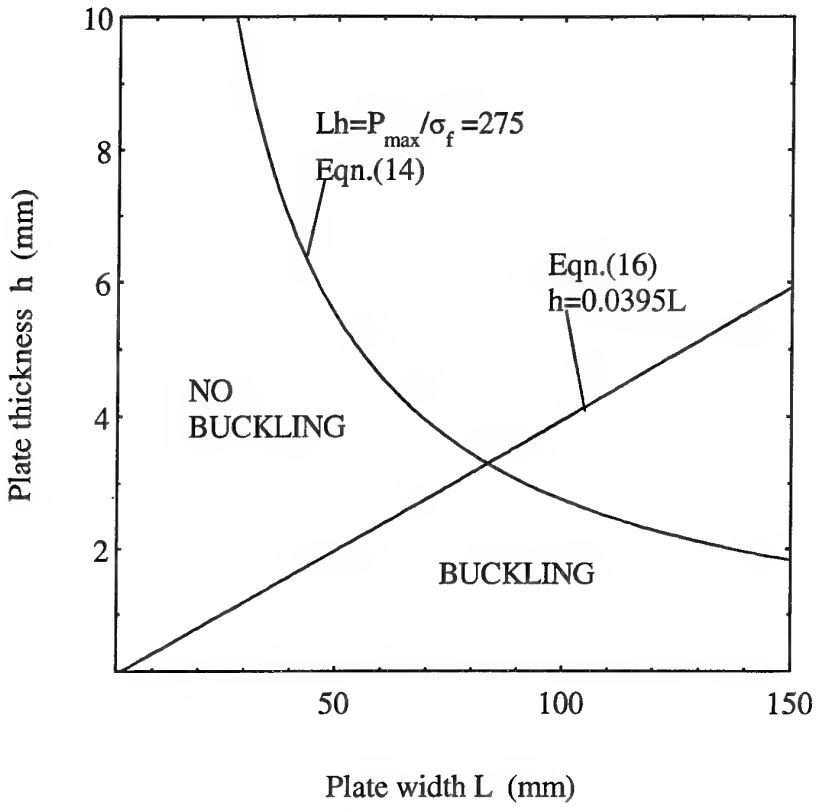

Fig.25 Design limits for a cruciform specimen to avoid buckling.

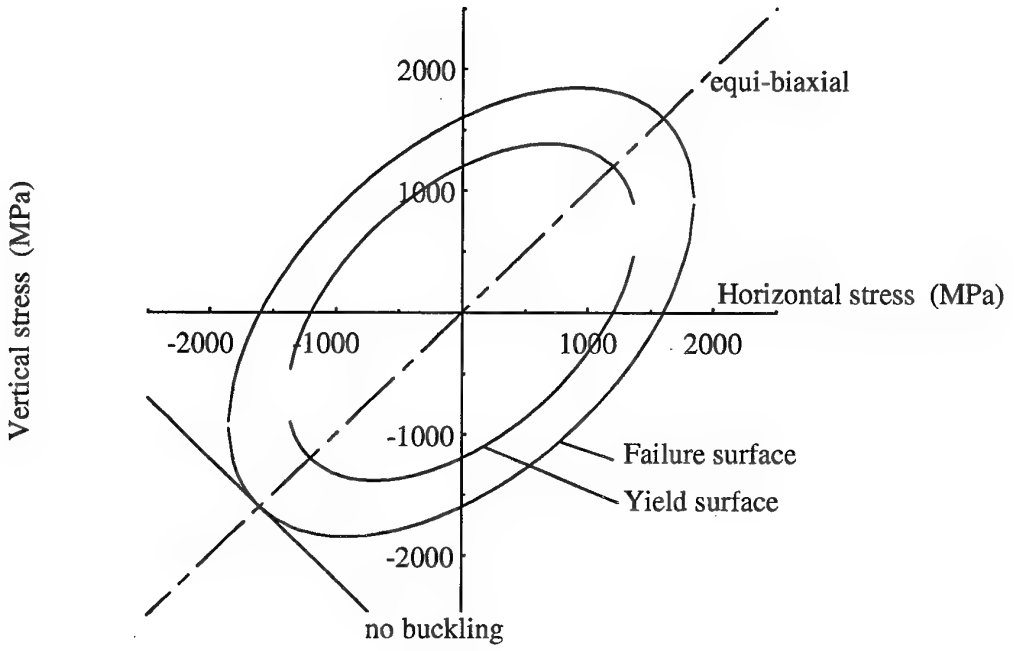

Fig.26 Yielding, failure, and buckling loci of modified cruciform specimens.

DISTRIBUTION LIST

Experimental Results of Cruciform Specimens under Biaxial Elastic-Plastic Loading

C.H. Wang and M. Heller

AUSTRALIA

DEFENCE ORGANISATION

S&T Program

Chief Defence Scientist
FAS Science Policy
AS Science and Industry and External Relations
AS Science Corporate Management
} shared copy

Counsellor Defence Science, London (Doc Data Sheet)
Counsellor Defence Science, Washington (Doc Data Sheet)
Scientific Adviser to Thailand MRDC (Doc Data Sheet)
Senior Defence Scientific Adviser/Scientific Adviser Policy and Command (shared copy)
Navy Scientific Adviser (3 copies Doc Data Sheet, 1 one copy distribution list)
Scientific Adviser - Army (Doc Data Sheet and distribution list only)
Air Force Scientific Adviser
Director Trials

Aeronautical and Maritime Research Laboratory

Director
Chief, AED
Research Leader
F. Rose
C.H. Wang (10 copies)
M. Heller (10 copies)
J. Paul
A. Searl

Electronics and Surveillance Laboratory

Director

DSTO Library

Library Fishermens Bend
Library Maribyrnong
Library DSTOS (2 copies)
Library, MOD, Pyrmont (Doc Data sheet only)

Forces Executive

Director General Force Development (Sea) (Doc Data Sheet only)
Director General Force Development (Land) (Doc Data Sheet only)
Director General Force Development (Air)
Director General Force Development (Joint) (Doc Data Sheet only)

Army
ABCA Office, G-1-34, Russell Offices, Canberra

Air Force
OIC ASI-LSA, DTA, HQLC (Sponsor)
Aircraft Research and Development Unit
Tech Reports, CO Engineering Squadron, ARDU
OIC ATF, ATS, RAAFSIT, WAGGA

S&I Program
Defence Intelligence Organisation
Library, Defence Signals Directorate (Doc Data Sheet only)

B&M Program (libraries)
OIC TRS, Defence Central Library
Officer in Charge, Document Exchange Centre (DEC), 1 copy
DEC requires the following copies of public release reports to meet exchange agreements under their management:
*US Defence Technical Information Centre, 2 copies
*UK Defence Research Information Centre, 2 copies
*Canada Defence Scientific Information Service, 1 copy
*NZ Defence Information Centre, 1 copy
National Library of Australia, 1 copy

UNIVERSITIES AND COLLEGES

Australian Defence Force Academy
Library
Head of Aerospace and Mechanical Engineering
Deakin University, Serials Section (M list)), Deakin University Library, Geelong, 3217
Senior Librarian, Hargrave Library, Monash University
Librarian, Flinders University
Librarian, Melbourne University

OTHER ORGANISATIONS

NASA (Canberra)
AGPS

OUTSIDE AUSTRALIA

ABSTRACTING AND INFORMATION ORGANISATIONS
INSPEC: Acquisitions Section Institution of Electrical Engineers
Library, Chemical Abstracts Reference Service
Engineering Societies Library, US
American Society for Metals
Documents Librarian, The Center for Research Libraries, US

INFORMATION EXCHANGE AGREEMENT PARTNERS
Acquisitions Unit, Science Reference and Information Service, UK
Library - Exchange Desk, National Institute of Standards and Technology, US
National Aerospace Laboratory, Japan
National Aerospace Laboratory, Netherlands

SPARES (10 copies)

Total number of copies: 80

DEFENCE SCIENCE AND TECHNOLOGY ORGANISATION
DOCUMENT CONTROL DATA

1. PRIVACY MARKING/CAVEAT (OF DOCUMENT)

2. TITLE

Experimental Results of Cruciform Specimens under Biaxial Elastic-Plastic Loading

3. SECURITY CLASSIFICATION (FOR UNCLASSIFIED REPORTS THAT ARE LIMITED RELEASE USE (L) NEXT TO DOCUMENT CLASSIFICATION)

Document	(U)
Title	(U)
Abstract	(U)

4. AUTHOR(S)

C.H. Wang and M. Heller

5. CORPORATE AUTHOR

Aeronautical and Maritime Research Laboratory
PO Box 4331
Melbourne Vic 3001

6a. DSTO NUMBER	6b. AR NUMBER	6c. TYPE OF REPORT	7. DOCUMENT DATE
DSTO-TR-0399	AR-009-808	Technical Report	August 1996

8. FILE NUMBER	9. TASK NUMBER	10. TASK SPONSOR	11. NO. OF PAGES	12. NO. OF REFERENCES
M1/9/111/1	95/228	AIR	43	11

13. DOWNGRADING/DELIMITING INSTRUCTIONS

None

14. RELEASE AUTHORITY

Chief, Airframes and Engines Division

15. SECONDARY RELEASE STATEMENT OF THIS DOCUMENT

Approved for public release

OVERSEAS ENQUIRIES OUTSIDE STATED LIMITATIONS SHOULD BE REFERRED THROUGH DOCUMENT EXCHANGE CENTRE, DIS NETWORK OFFICE, DEPT OF DEFENCE, CAMPBELL PARK OFFICES, CANBERRA ACT 2600

16. DELIBERATE ANNOUNCEMENT

No limitations

17. CASUAL ANNOUNCEMENT Yes

18. DEFTEST DESCRIPTORS

biaxial stresses; inelastic stresses; plastic theory

19. ABSTRACT

Biaxial experiments have been conducted using cruciform specimens to generate elastic-plastic material deformation data. Such data is required to validate a multiaxial constitutive model which has been implemented in finite element analysis codes at AMRL. The elastic-plastic data have been obtained for two aircraft metallic materials namely: 7050 aluminium alloy and D6AC high strength steel. In this work some of the deficiencies in the existing biaxial test system at AMRL have been rectified, including the provision for strain control testing. It has been shown that for this type of work, a new specimen design is needed to allow a wider range of biaxial stress conditions to be investigated, and a suitable design is given herein. Furthermore, as an alternative to incremental plasticity models, a simple closed-form, integral solution has been developed and is presented for proportional, cyclic loading. Using this integral solution, good agreement between experimental results and the theoretical predictions has been obtained.